**NASA TECHNICAL NOTE**

NASA TN D-5496

NASA TN D-5496

# FLUCTUATING PROPERTIES OF TURBULENT BOUNDARY LAYERS FOR MACH NUMBERS UP TO 9

*by William D. Harvey, Dennis M. Bushnell,
and Ivan E. Beckwith*

*Langley Research Center
Langley Station, Hampton, Va.*

| 1. Report No.<br>NASA TN D-5496 | 2. Government Accession No. | 3. Recipient's Catalog No. |
|---|---|---|
| 4. Title and Subtitle<br>FLUCTUATING PROPERTIES OF TURBULENT BOUNDARY LAYERS FOR MACH NUMBERS UP TO 9 | | 5. Report Date<br>October 1969 |
| | | 6. Performing Organization Code |
| 7. Author(s)<br>William D. Harvey, Dennis M. Bushnell, and Ivan E. Beckwith | | 8. Performing Organization Report No.<br>L-6533 |
| 9. Performing Organization Name and Address<br>NASA Langley Research Center<br>Hampton, Va. 23365 | | 10. Work Unit No.<br>124-07-18-02-23 |
| | | 11. Contract or Grant No. |
| 12. Sponsoring Agency Name and Address<br>National Aeronautics and Space Administration<br>Washington, D.C. 20546 | | 13. Type of Report and Period Covered<br>Technical Note |
| | | 14. Sponsoring Agency Code |

15. Supplementary Notes

16. Abstract

Estimates of the variation in intensity of the longitudinal velocity fluctuations across hypersonic turbulent boundary layers at Mach numbers from 8.2 to 8.9 have been made. These estimates were based on experimental measurements of fluctuating density and pitot pressure in the nozzle-wall boundary layer of a shock tunnel. Also, it is shown that reasonable estimates of the root-mean-square values of the fluctuating velocity, density, and temperature for Mach numbers from 1.72 to 8.9 can be made by using a mixing-length approach. Comparisons with previous experimental data indicate that the intensity of these fluctuating quantities, expressed in terms of suitable normalizing parameters, may be essentially independent of Mach number up to about Mach 9.

| 17. Key Words Suggested by Author(s)<br>Velocity-fluctuation estimates<br>Mixing-length approach | 18. Distribution Statement<br>Unclassified — Unlimited | | |
|---|---|---|---|
| 19. Security Classif. (of this report)<br>Unclassified | 20. Security Classif. (of this page)<br>Unclassified | 21. No. of Pages<br>50 | 22. Price*<br>$3.00 |

# FLUCTUATING PROPERTIES OF TURBULENT BOUNDARY LAYERS

## FOR MACH NUMBERS UP TO 9

By William D. Harvey, Dennis M. Bushnell,
and Ivan E. Beckwith
Langley Research Center

## SUMMARY

Estimates of the intensity of the longitudinal velocity fluctuations across a hypersonic turbulent boundary layer have been made on the basis of experimental measurements of fluctuating density and pitot pressure. These data were obtained at the Cornell Aeronautical Laboratory in the boundary layer on the wall of a shock-tunnel nozzle at Mach numbers from 8.2 to 8.9. Both the fluctuating and mean density data were obtained from the intensity of light emitted by the interaction of an electron beam with the local airflow.

A review of previous hot-wire data and assessment of the new data indicate that reasonable estimates of both the magnitude and trends of the intensity of fluctuating density, velocity, and temperature can be made by application of a simple mixing-length concept to mean flow data. Comparison of the new results with the previous hot-wire data indicates that the root-mean-square values of these fluctuating quantities may be essentially independent of Mach number up to about Mach 9, provided that suitable normalizing parameters are used.

## INTRODUCTION

Most of the available experimental data on compressible turbulent boundary layers is limited primarily to the mean properties of the flow. In order to obtain a better understanding of such boundary layers and ultimately advance theoretical prediction methods, it is necessary to study the statistical properties of the flow.

Measurements of mass flow and total temperature fluctuations in supersonic turbulent shear layers have been made with hot wires (see refs. 1 to 3). Root-mean-square levels of density, static temperature, and velocity fluctuations were obtained from these hot-wire data by applying a small-perturbation analysis and neglecting static pressure fluctuations. Direct measurements of density fluctuations and mean density have been made in hypersonic turbulent wakes by the use of electron-beam (ref. 4) and interferometric (ref. 5) techniques. Recent measurements of the mean and fluctuating density and

pitot pressure across a turbulent boundary layer on a shock-tunnel wall at a nominal Mach number of 8.5 were made at Cornell Aeronautical Laboratory and have been reported in reference 6. The density and pitot-pressure fluctuation data used herein were obtained from the original analog records for the Cornell Aeronautical Laboratory research. The purpose of the present paper is to estimate the intensity of the velocity fluctuations from these data of reference 6. Also an evaluation of a mixing-length approach to compute the magnitude and trend of the density and velocity fluctuations from data of reference 6 and other compressible data is made. Finally, comparisons are made with previous fluctuation measurements in zero-pressure-gradient boundary layers to determine whether any Mach number or Reynolds number effects can be established.

## SYMBOLS

A       second-order density-velocity correlation coefficient defined in equation (8)

$$a = (\gamma - 1)\overline{M}^2$$

$$b = \alpha\left(1 + \frac{\gamma - 1}{2}\overline{M}^2\right)\left(1 - \frac{T_w}{T_t}\right)$$

$$c = \frac{\overline{q'^2}}{\overline{u'^2}}$$

$c_p$       specific heat at constant pressure

G       function of Mach number defined in equation (5)

H       total enthalpy

h       static enthalpy

$l$       mixing length

M       Mach number

n       exponent in equation (B2)

$$P = \frac{\sqrt{\overline{p_t'^2}}}{\bar{p}_t}$$

$p$            pressure

$p_t$           pitot pressure

$$q = \left(\bar{u}^2 + 2\bar{u}u' + q'^2\right)^{1/2}$$

$$q' = \left(u'^2 + v'^2 + w'^2\right)^{1/2}$$

$R$           gas constant

$R_{Tu}$          second-order temperature-velocity correlation coefficient, $\dfrac{\overline{T'u'}}{\sqrt{\overline{T'^2}}\sqrt{\overline{u'^2}}}$

$R_{uq^2}, R_{\rho u^2}, R_{\rho q^2}, R_{\rho^2 u}$          third-order correlation coefficients defined in equations (C2)

$R_\delta$          Reynolds number based on boundary-layer thickness

$$r = \frac{\sqrt{\overline{\rho'^2}}}{\bar{\rho}}$$

$s$           distance along streamline

$T$           temperature

$T_t$          local stagnation temperature

$t$           stagnation point downstream of normal shock

$$U = \frac{\sqrt{\overline{u'^2}}}{\bar{u}}$$

$u, v, w$         longitudinal, normal, and transverse velocity components, respectively

$$u_\tau = \sqrt{\frac{\tau_w}{\rho_w}}$$

$x$           longitudinal coordinate

$y$           normal distance from tunnel wall

$\alpha$          angle between local fluctuating velocity vector and pitot tube axis

$\gamma$          specific heat ratio

$\delta$          nominal boundary-layer thickness

$\mu$          viscosity

$\rho$          density

$\tau$          shear stress

Subscripts:

aw          adiabatic wall

e          mean values at edge of boundary layer

o          settling chamber conditions

s          edge of sublayer as denoted by peak in $\sqrt{\overline{u'^2}}$ or in static values

w          wall conditions

$\alpha$          pitot-tube angle of attack

1,2          conditions ahead of and behind normal shock, respectively

A bar over a symbol indicates a time mean value. A prime denotes a fluctuating quantity.

## APPARATUS AND EXPERIMENTS

### Tunnel and Test Conditions

Measurements of density and pitot pressure were made in the turbulent boundary layer on the nozzle wall of the Cornell Aeronautical Laboratory 48-inch hypersonic shock tunnel (the actual diameter of the nozzle at the data station was about 23.5 inches or 0.597 meter). Data were obtained at a nominal Mach number of 8.5, and measurements of skin friction, heat transfer, and pressure on the nozzle wall were made simultaneously (ref. 6). All boundary-layer-profile measurements were made at a single station 135 inches (3.429 meters) downstream of the nozzle throat. A summary of the test conditions for the experimental program is provided in reference 6 where the free-stream conditions in the test section were calculated by assuming equilibrium air expansion to

the Mach number corresponding to the measured test-section pitot pressure. For convenience, these test conditions from reference 6 for the four runs used herein are listed in the table which follows (in the notation of the present paper). The assumption of equilibrium expansion can be justified on the basis of data reported in reference 7.

| $T_o$ | | $p_o$ | | $p_w$ | | $p_t$ | | $M_e$ | $T_e$ | | Free-stream Reynolds number per foot (per 30.5 cm) |
|---|---|---|---|---|---|---|---|---|---|---|---|
| °R | °K | psia | MN/m$^2$ | psia | N/m$^2$ | psia | N/m$^2$ | | °R | °K | |
| 5805 | 3225 | 845 | 5.8 | ≈0.035 | ≈241 | 3.30 | 22 752 | 8.25 | 502 | 279 | $1.52 \times 10^5$ |
| 3795 | 2108 | 240 | 1.6 | ≈.0115 | ≈79 | 1.10 | 7 584 | 8.62 | 272 | 151 | 1.10 |
| 2920 | 1622 | 290 | 2.0 | ≈.0125 | ≈86 | 1.29 | 8 894 | 8.89 | 189 | 105 | 2.12 |
| 3590 | 1994 | 385 | 2.6 | ≈.016 | ≈110 | 1.61 | 11 100 | 8.82 | 245 | 136 | 1.84 |

## Instrumentation

The mean and fluctuating density measurements were obtained with a 40-kilovolt electron-beam density probe which was projected through an orifice in the nozzle wall. A graphite cup was used to collect the beam current of approximately 1 milliampere. Photomultipliers were used to detect the fluorescent light emitted from collisions between the gas molecules and the beam electrons. A discussion of the design, operation, and calibration of the electron beam is included in the appendix of reference 6.

The mean and fluctuating pitot pressures were obtained by using piezoelectric crystals mounted in 0.125-inch-diameter (0.003175-meter) pitot tubes which were covered with protective caps. There was a small volume of gas between the crystals and the caps which had a small orifice to transmit the stagnation-pressure pulse to the crystals. A more complete discussion of the pitot probes used may be found in reference 6. Several possible types of interference between probes or between the viewing optics port and the wall instrumentation were evaluated, and the results of the evaluation may also be found in reference 6. The recording system, which was used to obtain the pitot data, sampled a given signal every 50 microseconds, stored it on a drum, and afterwards displayed the signal on a strip-chart recorder.

## CALCULATION OF FLUCTUATING QUANTITIES

### Mixing-Length Equations

A mixing-length formulation has been used to model temperature and velocity fluctuations for incompressible flow (refs. 8 and 9, for example) and velocity fluctuations

for compressible flow (ref. 10). An analogous mixing-length relation for the root-mean-square fluctuating density may be written as

$$\frac{\sqrt{\overline{\rho'^2}}}{\overline{\rho}} = \frac{l}{\delta}\frac{\rho_e}{\overline{\rho}}\left|\frac{d(\overline{\rho}/\rho_e)}{d(y/\delta)}\right| \tag{1}$$

Similarly, the root-mean-square fluctuating temperature may be expressed as

$$\frac{\sqrt{\overline{T'^2}}}{T_e} \approx \frac{l}{\delta}\left|\frac{d(\overline{T}/T_e)}{d(y/\delta)}\right| \cdot \tag{2}$$

and the root-mean-square fluctuating velocity, as

$$\frac{\sqrt{\overline{u'^2}}}{u_e} = \frac{l}{\delta}\left|\frac{d(\overline{u}/u_e)}{d(y/\delta)}\right| \tag{3}$$

where for the present purposes Prandtl's mixing-length concept is used in the inner portion of the boundary layer — that is,

$$l = 0.4y \qquad \left(0 \leq \frac{y}{\delta} \leq 0.2\right)$$

Recent calculations (refs. 9 and 10) indicate that the distribution for $l$ in the outer part of the boundary layer can be approximated as

$$l = 0.08\delta \qquad \left(0.2 \leq \frac{y}{\delta} \leq 1.0\right)$$

Slopes of the profiles of mean density, temperature, or velocity are used herein with equations (1), (2), or (3) to compute fluctuating values.

### Expressions for Velocity Fluctuations

The extension to compressible flow of recent calculation methods for incompressible flows that utilize the turbulent-kinetic-energy equation (refs. 11, 12, and 13) is to a large extent dependent upon a knowledge of the fluctuating quantities for compressible flow. Both the magnitude and distribution of the root-mean-square fluctuating velocities in a turbulent boundary layer are important parameters required in such methods.

A general relation (see appendix A) between the instantaneous velocity vector, density, and pitot pressure for values of $\alpha$ up to about $10^0$ may be written as

$$\rho_1 q_1^2 = G(M_1)p_t \tag{4}$$

where for constant density from the shock to the stagnation point

$$G\left(M_1\right) = \left(1 + \frac{p_1}{\rho_1 q_1^2} - \frac{1}{2}\frac{\rho_1}{\rho_2}\right)^{-1}$$  (5)

This function is compared with the exact solution for $G\left(M_1\right)$ in figure 1 where it is seen that for $M_1 > 2$ both relations give small changes in $G$ for large changes in Mach number. In the following derivation the fluctuating part of $G$ is therefore neglected. It is important to note that fluctuations in $p$ are not as yet neglected except through their effect on the $G$ function which is nearly constant for large changes in flow quantities.

Equation (4) is now applied to fluctuating turbulent flow, where in general the magnitude of $q_1$ is not the same as $u_1$, by assuming that the equation is correct for the instantaneous flow quantities. Substituting mean and fluctuating quantities for these instantaneous values in equation (4) and taking the time mean then gives

$$\frac{\overline{G}\overline{p}_t}{\overline{\rho}\overline{u}^2} = 1 + \frac{\overline{q'^2}}{\overline{u}^2} + 2\frac{\overline{\rho'u'}}{\overline{\rho}\overline{u}}$$  (6)

where it has been assumed that $\overline{v} = \overline{w} = 0$ so that $q^2 = \overline{u}^2 + 2\overline{u}u' + q'^2$. Note that the subscript $1$ has been dropped and that third- and higher order products of fluctuating quantities are neglected in equation (6) and in the following equations. If a suitable relation between $\overline{u'^2}$ and $\overline{q'^2}$ could be provided, equation (6) could be solved for $\sqrt{\overline{u'^2}}$ by using a correlation-coefficient form for $\overline{\rho'u'}$. However, the dependence on $\overline{q'^2}$, as well as on the mean flow quantity $\overline{G}\overline{p}_t/\overline{\rho}\overline{u}^2$, can be eliminated by utilizing the additional experimental data for $\overline{p_t'^2}$. That is, by first squaring both sides of equation (4), substituting mean and fluctuating quantities, and finally taking the time mean, the following equation is obtained:

$$\frac{\overline{G}^2\overline{p}_t^2}{\overline{\rho}^2\overline{u}^4}\left(1 + \frac{\overline{p_t'^2}}{\overline{p}_t^2}\right) = 1 + 4\frac{\overline{u'^2}}{\overline{u}^2} + 2\frac{\overline{q'^2}}{\overline{u}^2} + 8\frac{\overline{\rho'u'}}{\overline{\rho}\overline{u}} + \frac{\overline{\rho'^2}}{\overline{\rho}^2}$$  (7)

The quantity $\left(\dfrac{\overline{G}\overline{p}_t}{\overline{\rho}\overline{u}^2}\right)^2$ is then eliminated by the use of equation (6), and the second-order correlation coefficient

$$A = \frac{\overline{\rho'u'}}{\left(\overline{\rho'^2}\,\overline{u'^2}\right)^{1/2}}$$  (8)

7

is introduced. The resulting expression for the intensity of the fluctuating velocity may be written as

$$U = \frac{-Ar + \sqrt{A^2 r^2 + P^2 - r^2}}{2} \tag{9}$$

where only second-order products of fluctuation quantities are retained. It may be noted that $U$ is a function only of $P$ and $r$ (the ratios of mean-square fluctuations to mean values of pitot pressure and density, respectively) and of the correlation coefficient $A$. The effect on $U$ of the likely range of values for the coefficient $A$ is evaluated in appendix B. As mentioned previously, the magnitude of the fluctuating vector $q'$ does not appear in this final equation. Also, a relation identical to that of equation (9) is obtained if $q_1$ is replaced by $u_1$ in equation (4) and if all terms of third and higher order are consistently neglected (see ref. 14). It can therefore be concluded that to the order of approximation used in equation (9), the fluctuations in mass flow caused by the cross velocity components $v'$ and $w'$ have no effect on $P$ in spite of the fact that, in general, the magnitude of the instantaneous vector $q$ is not equal to $u$.

If third-order terms are retained in the derivation, certain third-order correlations involving $q'$, $u'$, and $\rho'$ are present in the final equation for $U$. The effect of these third-order correlations on $U$ is evaluated in appendix C. It is shown in appendix C that over the maximum possible range for these third-order correlations, a maximum uncertainty of about $\pm 20$ percent in predicted values of $U$ is possible.

A second and more simplified method to derive an approximate relation between the fluctuating velocity vector, density, and pitot pressure is to take the derivative of the log of equation (4) $\left(\text{with } q^2 = u^2 + v^2 + w^2\right)$ which gives

$$\frac{d\rho}{\rho} + 2\frac{u\,du}{q^2} + 2\frac{v\,dv}{q^2} + 2\frac{w\,dw}{q^2} = \frac{dG}{G} + \frac{dp_t}{p_t} \tag{10}$$

Then, as in reference 3, for example, the differential quantities are considered the same as the corresponding fluctuating quantities, and all other quantities are considered as mean values. After squaring both sides and taking the time mean, equation (10) may be written as

$$\frac{\overline{\rho'^2}}{\bar{\rho}^2} + 4\frac{\overline{\rho'u'}}{\bar{\rho}\bar{u}} + 4\frac{\overline{u'^2}}{\bar{u}^2} = \frac{\overline{p_t'^2}}{\bar{p}_t^2} \tag{11}$$

After the introduction of the coefficient $A$, the solution of equation (11) for $U$ is identical to equation (9).

The only limitations to the generality of equation (9) are that fluctuation terms of third and higher order are neglected and that $\frac{G'}{\bar{G}} \ll 1.0$. From figure 1, this latter assumption restricts the use of equation (9) to conditions where $M_1 > 2.0$; that is, the equation can be used over all the hypersonic turbulent boundary layer except near the wall $\left(M_1 < 2\right)$. The data of reference 6 indicate that the local Mach number is about 2.5 at a value of $y/\delta$ of approximately 0.05. Therefore application of equation (9) to the data of reference 6 is expected to be valid for $\frac{y}{\delta} \geqq 0.05$.

## RESULTS AND DISCUSSION

### Measurements of Density and Pitot-Pressure Fluctuations at Mach 9

Figures 2 and 3(a) show the variations in the ratios of root-mean-square values of the density and pitot-pressure fluctuations (also shown in ref. 6) to the respective local mean values across the boundary layer. Figure 3(b) shows the ratio of the root-mean-square value of wall-pressure fluctuations to the mean dynamic pressure at the boundary-layer edge. The data in figures 2 and 3(a) and the data from reference 6 in figure 3(b) were computed at the Langley Research Center from the original oscilloscope records of the density and strip-chart records of pitot and wall pressures.

Under the assumption that the sensors used in reference 6 have a linear output over the range of a fluctuating signal, the ratios of the root-mean-square values of density and pitot-pressure fluctuations to the respective mean values are essentially independent of the absolute levels of density or pitot pressure. Consequently, the accuracy of the individual data points in figures 2 and 3(a) is believed to be better than the accuracy of the mean data as given in reference 6. The fluctuations of both density and pitot pressure increase rapidly near the wall. The density profiles near the wall indicate a definite peak which, by analogy with incompressible data, is presumably in the vicinity of the edge of the sublayer. The overall level of the pitot-pressure fluctuation is considerably higher than that of the density fluctuation because, as shown by equation (11), the fluctuating pressure depends essentially on the sum of the fluctuating density and velocity and on the correlation $\overline{\rho'u'}$, which is always positive as indicated in appendix B.

It should also be noted from figures 2 and 3(a) that a definite minimum in the distribution of the fluctuation intensities of both density and pitot pressure generally occurs at values of $y/\delta$ from about 0.2 to 0.5. Shown in figure 4(a) are the data points and faired distribution of the ratio of mean density to the density at the edge of the boundary layer as previously presented in reference 6. Presented in figure 4(b) are the same data but with a possible alternate fairing which is used herein. If it is assumed that the density fluctuations can be modeled by a mixing-length expression as previously discussed,

then the "flattening out" in the faired mean density profiles shown in figure 4(b) would imply a minimum in the density fluctuation profiles at about the same locations as shown in figure 2. It is of further interest to note that similar "flat" regions in static temperature profiles have previously been reported (ref. 15) and have been observed in data for a turbulent boundary layer on the wall of a Mach 8 tunnel at the Langley Research Center.

The intensity of fluctuation in the wall static pressure $\sqrt{\overline{p_w'^2}}\big/\bar{p}_w$ obtained from the original records is plotted in figure 3(a) (see solid symbols). If the limiting value of $\sqrt{\overline{p_t'^2}}\big/\bar{p}_t$ at $y = 0$ is this quantity, then the data of figure 3(a) indicate that the peaks in the pitot-pressure fluctuations are very sharp and close to the wall. These wall-static-pressure data were obtained with the same type of transducer used for the pitot-pressure measurements; however, attenuation of the fluctuating wall pressure may have occurred to a greater extent than that of the pitot pressure. This greater attenuation might be expected because of the lower absolute level in static pressure and differences in volume and lengths of tubing connecting the transducers to the pressure orifices.

The fluctuations in wall static pressure are compared with previous data in figure 3(b) where $\sqrt{\overline{p_w'^2}}\big/\frac{1}{2}\rho_e u_e^2$ is plotted as a function of $M_e$. The data in this figure are from a number of different sources and are shown here as presented in figure 4 of reference 16 except that the data from reference 6 and the line attributed to Laufer (ref. 17) have been added. This line was obtained directly from lines faired through the mean of the data of figures 2 and 3 in reference 17; $\sqrt{\overline{p_e'^2}}\big/\frac{1}{2}\rho_e u_e^2$ was obtained from figure 2 and $\sqrt{\overline{p_w'^2}}\big/\sqrt{\overline{p_e'^2}}$ from figure 3 of that reference. The present data (from ref. 6) are lower than all other data; however, the indicated trend with Mach number is consistent with the available data.

As a further check on the level of data for $\sqrt{\overline{p_w'^2}}$, the correlation equation

$$\frac{\sqrt{\overline{p_w'^2}}}{\frac{1}{2}\rho_e u_e^2} = 0.006 \frac{\bar{\rho}_s}{\bar{\rho}_e} \tag{12}$$

may be derived from the equation $\sqrt{\overline{p_w'^2}} \approx 0.006 \frac{1}{2}\rho u_e^2$ for incompressible flow (from ref. 18, given in notation of present paper) by replacing the constant density $\rho$ with the mean density at the edge of the sublayer. Equation (12) has been evaluated for adiabatic wall temperatures and for the cold wall temperatures of reference 6, and the results are shown in figure 3(b). It is seen that most of the previous data which were for adiabatic wall conditions are below the adiabatic-wall correlation-equation line and that the data

10

of reference 6 are considerably below the corresponding cold-wall correlation-equation values. Values of $\bar{\rho}_s/\rho_e$ used in these cold-wall estimates were taken as 0.35 to 0.6 from figure 4(b).

### Evaluation of Mixing-Length Approach

A comparison of the root-mean-square density fluctuations computed by equation (1) $\left(\text{where the values of } \dfrac{d(\bar{\rho}/\rho_e)}{d(y/\delta)} \text{ were taken from fig. 4(b)}\right)$ with the experimental data of reference 6 is shown in figure 5. The bands include all data from the four test runs indicated in figure 2. In general, the mixing-length approach predicts the intensity of the density fluctuations to within about a factor of 2.

The root-mean-square temperature fluctuations of Kovásznay (ref. 2) and of Kistler (ref. 3) have also been compared with calculations obtained by a mixing-length approach. Calculations of the fluctuating temperature data, shown in figure 6(a) for reference 2 and figure 6(b) for reference 3, were made by using the slopes of the mean temperature data and equation (2). The total temperature through the boundary layer was taken to be constant for reference 2 in forming the fluctuation temperature ratio $\sqrt{\overline{T'^2}}/T_e$ (see fig. 6(a)). The mean total temperature and the mean velocity distributions across the boundary layer were used to reduce the data of reference 3 shown in figure 6(b) for $1.72 \leqq M_e \leqq 4.67$. For both sets of data the mixing-length approach generally predicted the intensity of the temperature fluctuations to within somewhat better than a factor of 2.

A comparison of the root-mean-square velocity fluctuations computed by equation (3) with those computed by equation (9) for the data of reference 6 are shown in figure 7. Both hatched bands include all computed points from the four test runs. Velocity derivatives were obtained from fairings of mean-velocity profiles shown in figure 8. These velocity profiles were computed from the faired density profiles of figure 4(b) and the original data for $\bar{p}_t$ in reference 6. Results from equation (9) were obtained from the fluctuation intensity distributions of figures 2 and 3 with $A = 1.0$ and with $\bar{u}/u_e$ from figure 8. These results from equation (9) are discussed in more detail in the next section. The mixing-length approach (eq. (3)) predicts velocity fluctuation intensities that are roughly a factor of 3 larger than the results calculated from equation (9).

The root-mean-square velocity fluctuations of Kovásznay (ref. 2) and Kistler (ref. 3) have also been computed from the mixing-length equation (eq. (3)). The results of these computations are compared with measured values in figure 9 where the mean velocity data through the boundary layer were taken from the respective references. The bands for the reference 3 results (see fig. 9) are representative of three tests $(1.72 \leqq M_e \leqq 4.67)$. For both sets of data (refs. 2 and 3), the mixing-length calculations again are correct to within a factor of 2.

L

## Correlations of Root-Mean-Square Velocity Fluctuation

Distributions across the boundary layer.- Figure 10 shows the longitudinal velocity fluctuation intensities determined from equation (9) by using the distributions of fluctuation quantities in figures 2 and 3 and $A = 1.0$. In appendix B it is shown that the coefficient $A$ should be positive and values of $A$ would be expected to range from about 0.5 to 1.0; calculations in appendix B indicate a maximum effect on $\sqrt{\overline{u'^2}}/\bar{u}$ of $\pm 10$ percent for this range of $A$ values. The ratios of $\sqrt{\overline{u'^2}}/u_e$ (fig. 10) were obtained by utilizing the $\bar{u}/u_e$ values shown in figure 8. Also shown for comparison in figure 10 are data obtained by hot-wire techniques (refs. 3, 19, and 20). The line shown in figure 10 for reference 3 represents a mean of data at three different Mach numbers; only one line is shown because the data were correlated to within a relatively narrow band by the use of $u_e$ rather than $u_\tau$ as the normalizing parameter. To illustrate this improved correlation, the data of reference 3 normalized with respect to $u_\tau$ are plotted in figure 11(a) as originally presented in reference 3, and the same data normalized with respect to $u_e$ are plotted for comparison in figure 11(b). The data are correlated to within about 30 percent over the entire boundary layer by the use of $u_e$. This improved correlation indicates that the root-mean-square velocity fluctuations normalized by the external velocity may be independent of Mach number and should probably be used instead of the local energy of longitudinal fluctuations normalized by the wall shear stress as proposed by Morkovin in reference 1.

In figure 10 it can be seen that near the wall the velocity fluctuation levels for the present data from reference 6 (from eq. (9)) show a large increase to a peak value that is presumably in the vicinity of the sublayer edge and that appears to be somewhat farther from the wall than the peak values for the low-speed data of references 19 and 20. In the outer portion of the boundary layer $\left(\frac{y}{\delta} > 0.6\right)$ the present results are in reasonable agreement with previous data. The theory of reference 13 predicts an inverse relationship between $\sqrt{\overline{u'^2}}/u_e$ and $R_\delta$; thus it might be expected that the results from reference 6 should be at a higher level (for the same $y/\delta$) than the data of references 3 and 20 since values of $R_\delta$ for the data of reference 6 are smaller. However, the present results in the range $0.2 \le \frac{y}{\delta} \le 0.6$ are lower than previous data, either because of a Mach number or wall-temperature effect or because of some anomaly in the experimental conditions of reference 6. The trends shown in figure 10 are again largely dependent upon the trends of the fluctuating data in figures 2 and 3(a), which were used to compute the fluctuating velocity. If the trends shown for these fluctuating data are realistic, then possible explanations for the smaller values of $\sqrt{\overline{u'^2}}/u_e$ noted may be as follows: (1) The smaller values may result from finite flow disturbances which could affect the mean profiles upstream of the test section; or (2) the large favorable pressure gradients upstream

of the test section may have reduced the value of $\sqrt{\overline{u'^2}}/u_e$. That is, the midregion of the boundary-layer profiles from reference 6 may not be representative of flat-plate turbulent-boundary-layer flows. If the data in this region are considered atypical, the general agreement elsewhere between the present Mach 9 results and the previous lower Mach number data (fig. 10) indicates that Morkovin's hypothesis in reference 1 (that the basic turbulent mechanisms are independent of Mach number) can provisionally be extended to the lower range of hypersonic Mach numbers and cold wall conditions.

Variation with Reynolds number.- In comparing the available longitudinal velocity fluctuation data at different Mach numbers in the present report, an attempt was made to use data taken at similar values of $R_\delta$ so that the effect of Mach number could be determined independent of any Reynolds number effects. It would also be of interest to examine the available velocity fluctuation data, most of which is at subsonic speeds, for any effect of $R_\delta$, both for use in a comparison with the prediction method of reference 13 and for possible later extrapolation to higher speeds.

The results obtained from a survey of the available data (from refs. 2, 3, 6, and 19 to 38) are shown in figure 12. Values of the Mach number are inserted next to the data points when the Mach number is appreciably different from zero. Shown for comparison with the data are predictions of reference 13 for incompressible flow on a flat plate. Since the computed quantity in reference 13 is total turbulent kinetic energy, some relation between $\sqrt{\overline{u'^2}}$ and the other turbulent velocity components must be postulated before a prediction of $\sqrt{\overline{u'^2}}$ can be made. For the near-wall region, the data of reference 19 indicate that a reasonable relation is $\overline{q'^2} = 1.5\overline{u'^2}$, which gives the dashed lines (figs. 12(a) and 12(b)). The solid line (fig. 12(c)) is from the relation $\overline{q'^2} = 2\overline{u'^2}$ which, as indicated in reference 13, is a reasonable approximation for the outer region of an incompressible turbulent boundary layer.

Peak values of the velocity fluctuation data normalized with respect to $u_\tau$ (where $u_\tau$ values could be obtained with certainty) are plotted as functions of $R_\delta$ in figure 12(a). Most of the data are within about 20 percent of the level predicted in reference 13 except for the present data, the data from references 34 and 38, and some data from reference 25 $\left(\text{occurring between } 5 \times 10^3 \lesssim R_\delta \lesssim 2 \times 10^4\right)$ which are believed to have been obtained in transitional flow. The present Mach 9 results from reference 6 $\left(5 \times 10^4 \lesssim R_\delta \lesssim 8 \times 10^4\right)$ fall on the lower side of the data scatter. These data points were obtained from the peak values of $\sqrt{\overline{u'^2}}$ as computed with equation (9) for the runs of reference 6 for which surface shear data were available. It is seen that in spite of the high Mach numbers and cold wall conditions, these data are in reasonable agreement with previous data which are for adiabatic wall conditions and a maximum Mach number of about 0.7. It should be noted, however, that the viscous sublayer is evidently much thicker for these low Reynolds number, Mach 9 data than for the low-speed data. That

is, if the thickness of the viscous sublayer is taken as $\left(\frac{y}{\delta}\right)_s \approx 0.1$, which corresponds to the approximate location of the peak in $\sqrt{\overline{u'^2}}/u_e$ for the present data (see fig. 10), the values of a law-of-the-wall coordinate $\frac{\rho_w u_\tau}{\mu_w} y_s$ range from about 60 to 120. The corresponding range of values in this coordinate for the low-speed data of figure 12(a) is from 15 to 20. When the effects of variable density are included by using the Baronti-Libby transformation theory (ref. 39), the values of the transformed law-of-the-wall coordinate for the present data at $\left(\frac{y}{\delta}\right)_s \approx 0.1$ are from about 40 to 70, again a range which indicates an unusually thick sublayer.

Velocity fluctuation data are usually normalized by $u_\tau$ rather than by $u_e$, and the ratio $\sqrt{\overline{u'^2}}/u_\tau$ has been found to be relatively invariant with Reynolds number at low speeds, as discussed for instance in reference 40 and shown in figure 12(a). However, figures 11(a) and 11(b) have indicated that the apparent effect of Mach number is reduced if the velocity fluctuation data are normalized by $u_e$ rather than by $u_\tau$, and therefore $\sqrt{\overline{u'^2}}/u_e$ may be a useful parameter for comparing low-speed data with data from compressible flows. The root-mean-square velocity fluctuation data at the peak and at $\frac{y}{\delta} = 0.5$ are plotted in this form in figures 12(b) and 12(c), respectively. Correlation of the peak values may be slightly better when $u_\tau$ is used (fig. 12(a)) than when $u_e$ is used (fig. 12(b)). In the latter plot the predicted trend of $\left(\frac{\sqrt{\overline{u'^2}}}{u_e}\right)_{peak}$ with $R_\delta$ is in agreement with the data. At $\frac{y}{\delta} = 0.5$ (fig. 12(c)) the data are not as well correlated as in the previous figures and the Mach 9 data are considerably lower than most of the previous data. The trend of the theoretical prediction (ref. 13) is supported by the data but the predicted level is too high. There appears to be no consistent variation with Mach number in figure 12(c); however, the Mach 9 results are low.

In view of the previous discussion concerning the detailed comparison of the $\sqrt{\overline{u'^2}}/u_e$ profile for $M \approx 9$ with lower Mach number data (fig. 10), the fact that the data for $M \approx 9$ at $\frac{y}{\delta} = 0.5$ are low (fig. 12(c)) probably does not invalidate the tentative extension of the hypothesis of reference 1 to hypersonic Mach numbers of about 9 for cold wall conditions and boundary layers with small pressure gradients.

Correlations of Root-Mean-Square Temperature or Density Fluctuations

The density fluctuation data from reference 6 (as presented herein) may be compared directly with temperature fluctuation data from other sources since, from the equation of state,

$$\frac{d\rho}{\rho} = -\frac{dT}{T} + \frac{dp}{p}$$

14

Then if the level of pressure fluctuations is neglected (see appendix B), the root-mean-square ratios of density and temperature are equal

$$\frac{\sqrt{\overline{\rho'^2}}}{\bar{\rho}} = \frac{\sqrt{\overline{T'^2}}}{\bar{T}}$$

In comparisons of $\sqrt{\overline{\rho'^2}}$ with previous data for $\sqrt{\overline{T'^2}}$, a normalizing parameter that would minimize variations caused by Mach number and wall temperature should be used. For velocity fluctuations it has been shown (figs. 10 and 11) that the appropriate normalizing parameter is $u_e$, which is the mean velocity at the edge of the boundary layer (i.e., the difference between the velocity at the wall and the edge). The same reasoning applied to the temperature or density fluctuations indicates that the normalizing parameter should be $T_w - T_e$ or $\rho_e - \rho_w$ for situations where the wall temperature or density is the maximum or minimum value, respectively, across the boundary layer such as for adiabatic or hot wall conditions. For cold wall conditions where heat is transferred to the wall from the boundary layer, there is a peak in temperature $T_s$ and a corresponding minimum in density $\rho_s$ very close to the wall. The normalizing parameter for these conditions should then be $T_s - T_e$ or $\rho_e - \rho_s$. Similar normalizing parameters (maximum velocity and density defects) were found to correlate velocity and density fluctuation data in a compressible wake flow (ref. 41).

To determine the effect of increasing Mach number for these normalizing parameters, the temperature fluctuation data of references 2, 3, and 26 have been normalized by the difference between their respective wall and boundary-layer-edge temperatures, and the results are plotted as functions of $y/\delta$ in figure 13 (note that $T_w \approx T_s$ for ref. 26 because $M \approx 0$). Similarly, the fluctuation density data of reference 6 have been normalized by the differences between the edge and minimum density and are also shown in figure 13 (the ideal gas values of $\rho_e$ from ref. 6 have been used). The dimensionless fluctuating density and temperature profiles shown from the various sources are in agreement within a factor of about 2 over most of the boundary layer. Consequently, the nominal trends and magnitudes shown in figure 13 are useful for estimates of fluctuation levels in both compressible and incompressible boundary layers.

CONCLUDING REMARKS

Estimates of the variation in intensity of the longitudinal velocity fluctuations across a hypersonic turbulent boundary layer at Mach numbers from 8.2 to 8.9 have been made by utilizing experimental measurements of fluctuating density and pitot pressure. Analysis of the momentum relation used to make these estimates indicates that when all third and higher order correlations of fluctuating quantities are neglected, the fluctuations in

mass flow normal to the mean velocity vector have no effect on fluctuations in pitot pressure.

Comparison of available data indicates that for the outer part of constant-pressure boundary layers, the root-mean-square values of the fluctuating velocity normalized by the mean velocity at the edge of the boundary layer may be independent of wall temperature and Mach number up to Mach 9. In the near-wall region where the intensity of velocity fluctuations reaches a maximum, the shear-stress velocity may be a more suitable normalizing parameter.

When the root-mean-square values of the density and temperature fluctuations across the boundary layer were normalized by the difference between the respective minimum or maximum mean value across the boundary layer and the mean value at the boundary-layer edge, available data were again found to be essentially independent of Mach number and wall temperature.

On the basis of these preliminary results, it appears that by the use of mixing-length concepts or appropriate correlating parameters, estimates can be made of trends and magnitudes, within a factor of 2, of fluctuating velocity, density, and temperature for Mach numbers up to about 9 and for cold wall conditions. The validity of the hypothesis that the basic turbulent mechanisms are independent of Mach number is thereby provisionally extended to cold wall conditions and to hypersonic Mach numbers of about 9.

Langley Research Center,
National Aeronautics and Space Administration,
Langley Station, Hampton, Va., August 1, 1969.

# APPENDIX A

## DERIVATION OF INSTANTANEOUS PITOT-PRESSURE EQUATIONS

An approximate relation between the fluctuating velocity, density, and pitot pressure may be derived by assuming that the usual steady-flow equations apply to the instantaneous pitot pressure. In this derivation the molecular shear is neglected and, for simplicity, the instantaneous density from the postshock point (point 2) to the stagnation point is assumed constant. For a conventional pitot tube at zero angle of attack as illustrated in the following sketch,
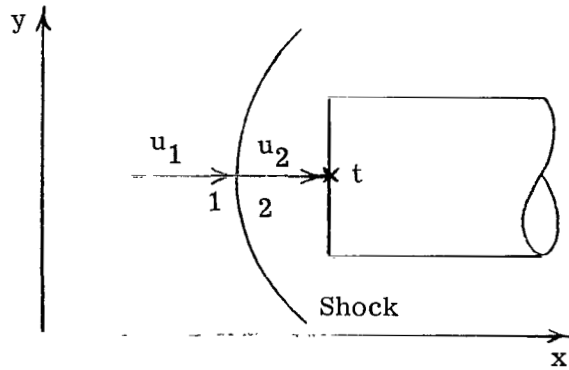


the instantaneous pitot pressure measured by the tube would be (as obtained from ref. 42, p. 243, for example, and given in the present notation)

$$p_t = \rho_1 u_1{}^2 \left( 1 + \frac{p_1}{\rho_1 u_1{}^2} - \frac{1}{2} \frac{\rho_1}{\rho_2} \right) \tag{A1}$$

If the pitot tube is placed at some angle of attack such that the instantaneous velocity vector ahead of the shock is $q_1$ and if the shock is assumed normal to $q_1$ as shown in the following sketch,
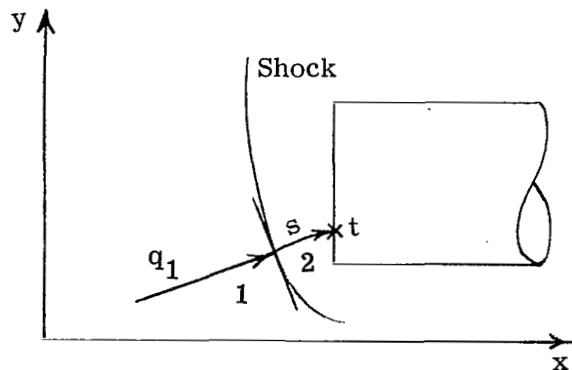
the measured pitot pressure will have the same dependence on the density and on the magnitude of the velocity vector as in equation (A1) since the entropy of the stagnation streamline is identical if $q_1 = u_1$. The following derivation (analogous to that of eq. (A1)) is included to illustrate this effect of angle of attack on pitot pressure.

Conservation of momentum across the shock requires that

$$p_1 + \rho_1 q_1^2 = p_2 + \rho_2 q_2^2 \tag{A2}$$

The momentum equation along a postshock streamline is

$$\rho q \frac{\partial q}{\partial s} = -\frac{\partial p}{\partial s} \tag{A3}$$

If the streamline shown in the preceding sketch is assumed to stagnate on the tube face at point t, then the measured pitot pressure is approximately (by integration of eq. (A3))

$$p_t = p_2 + \frac{\rho_2 q_2^2}{2} \tag{A4}$$

where again the instantaneous density from point 2 to point t is assumed constant. By eliminating $p_2$ from equations (A2) and (A4) and using the continuity equation $\rho_1 q_1 = \rho_2 q_2$, the following equation is obtained:

$$p_t = \rho_1 q_1^2 \left(1 + \frac{p_1}{\rho_1 q_1^2} - \frac{1}{2}\frac{\rho_1}{\rho_2}\right) \tag{A5}$$

Comparison of equations (A1) and (A5) shows that these equations are identical in terms of the local velocity vectors $u_1$ and $q_1$, as would be required by the assumption that the pitot-tube shock is normal to the stagnation streamline. The measured pitot pressure would therefore be insensitive to angle of attack as long as this assumption is valid and the magnitude of $q_1$ is the same as $u_1$. Experimental results of reference 43, for example, indicate that these assumptions are correct for pitot-tube angles of attack up to about 20° at Mach numbers up to 6, since the measured total pressure was essentially independent of angle of attack over this range of conditions.

To determine the effect of pitot-tube angle of attack at higher Mach numbers, some data were obtained at a Mach number of 19 in the Langley hypersonic nitrogen tunnel. These data are shown in figure 14 where the measured pitot pressures (normalized to the values at $\alpha = 0$) are plotted against angle of attack of the tube. (The experimental conditions for these data are given in the figure.) These data indicate that the effect of pitot-tube angle of attack on total pressure is about 7.5 percent at $\alpha = 20°$ for

$M_e = 19$. The increased effect of $\alpha$ at Mach 19, as compared with the effect at lower Mach numbers in reference 43, may not be entirely due to the increase in Mach number, since the pitot-tube lip shape was different for the two sets of data. The sharp-lip configuration of reference 43 is known to minimize the angle-of-attack effect, as indicated in reference 44. The blunt tip used for the Mach 19 data is more nearly like the pitot-tube tip used in reference 6. The data of figure 14 are therefore thought to more nearly represent the effect of $\alpha$ on $p_t$ for the conditions of reference 6.

# APPENDIX B

## EVALUATION OF SECOND-ORDER CORRELATION COEFFICIENT A

The purpose of this appendix is to show that definite limits on the values of the second-order correlation of fluctuation density and velocity (eq. (8)) can be established from the measurements of reference 6 for mean and fluctuating pitot pressure and density. It is shown that the values of $\overline{u'^2}$ are not overly sensitive to values of the corresponding correlation coefficient as prescribed by these limits.

### Preliminary Remarks

Morkovin (ref. 1) has shown, for boundary layers with zero heat transfer, the following temperature-velocity correlation coefficient (given here in the notation of the present paper):

$$R_{Tu} = \frac{\overline{T'u'}}{\sqrt{\overline{T'^2}}\sqrt{\overline{u'^2}}} \approx -1.0$$

This estimate has been verified to within about 50 percent by data of Morkovin at $M_e \approx 1.75$ (ref. 1) where $-0.9 < R_{Tu} < -0.7$ and by data of Kistler (ref. 3) where $-0.8 < R_{Tu} < -0.5$ up to Mach number 4.67. From the equation of state with negligible pressure fluctuations, the fluctuations in $\rho$ and $T$ are related by the expression

$$\frac{\rho'}{\bar{\rho}} = -\frac{T'}{\bar{T}}$$

By using this relation, it can be inferred that for adiabatic boundary layers, the values of the density-velocity correlation coefficient $A = \dfrac{\overline{\rho'u'}}{\left(\overline{\rho'^2}\,\overline{u'^2}\right)^{1/2}}$ would be in the same range as $R_{Tu}$ but of opposite sign. Although there are no direct measurements of static pressure fluctuations in a boundary layer, it is reasonable to neglect $\sqrt{\overline{p'^2}}/\bar{p}$, which is small compared with $\sqrt{\overline{\rho'^2}}/\bar{\rho}$, on the basis of the low levels of $\sqrt{\overline{p_w'^2}}/\bar{p}_w$ shown in figure 3(a) and the expectation that $\sqrt{\overline{p'^2}}$ would decrease by an order of magnitude from the wall value over most of the boundary layer. This rapid decrease in $\sqrt{\overline{p'^2}}$ with increasing $y$ in the near-wall region is consistent with the theory of reference 45 and with the data of Laufer (ref. 17), who found that free-stream values of $\sqrt{\overline{p'^2}}$ were one-tenth of the wall values.

The magnitude of A can be independently determined, since it can be reasoned as in reference 1 that for a region (even in a cold-wall boundary layer) where both $\partial \bar{p}/\partial y$ and $\partial \bar{u}/\partial y$ are positive, the correlation $\overline{\rho'u'}$ should be positive. That is, if a lump of gas with a smaller than average density came from a layer close to the wall, it would have a velocity smaller than average. Since the data of Wallace (ref. 6) satisfy these conditions on the mean flow gradients for most of the boundary layer as shown by figures 4 and 8, the values of A should be within the limits $0 \leqq A \leqq 1.0$.

## Basic Equations

Four independent relations between the instantaneous flow quantities are required in order to evaluate the coefficient A. The pitot-pressure relation (eq. (4)) has been derived in appendix A and its limitations discussed in the text. This equation may be written as

$$\rho q^2 = \rho\left(u^2 + v^2 + w^2\right) = G(M)p_t \tag{B1}$$

In place of the "Strong Reynolds Analogy" assumption used by Morkovin (ref. 1) for adiabatic walls, it is assumed herein that the relation

$$\frac{T_t - T_w}{T_{t,e} - T_w} = \left(\frac{u}{u_e}\right)^n \tag{B2}$$

represents a solution to the energy equation that accounts roughly for the effects of upstream pressure gradient and of Prandtl number not equal to 1.0. Equation (B2) should probably be used only for $\frac{u}{u_e} > 0.5$ and cold wall conditions. Values of n that might apply to instantaneous flow quantities are unknown, so for the present purposes it is further assumed that values of n corresponding to mean flow data can be used. That is, depending on the type of flow under consideration, n would generally be in the range

$$1.0 < n < 2.5$$

The other relations required are the equation of state

$$p = \rho RT \tag{B3}$$

and the definition of local stagnation temperature

$$T_t = T + \frac{u^2 + v^2 + w^2}{2c_p} \tag{B4}$$

It has been shown in the text (compare eqs. (10) and (11) with eq. (9)) that second-order correlation equations can be obtained directly from differential forms of the basic relations. Before applying this procedure to equations (B1) to (B4), it should be noted that multiplication of equation (B4) by $\rho R$ and the use of equation (B3) give

$$p + \frac{R}{2c_p} \rho\left(u^2 + v^2 + w^2\right) = R\rho T_t$$

By taking the log derivative of this equation and rearranging terms, the equation

$$\frac{dT_t}{\overline{T}} = \frac{dp}{\overline{p}} - \frac{d\rho}{\overline{\rho}} + (\gamma - 1)\overline{M}^2 \frac{du}{\overline{u}} \tag{B5}$$

is obtained when $\overline{v} = \overline{w} = 0$. Similarly from equation (B2) (for $T_w$ assumed constant)

$$\frac{dT_t}{\overline{T}} = n\left(1 + \frac{\gamma - 1}{2}\overline{M}^2\right)\left(1 - \frac{T_w}{T_t}\right)\frac{du}{\overline{u}} \tag{B6}$$

and from equation (B1)

$$\frac{dp_t}{\overline{p}_t} = \frac{d\rho}{\overline{\rho}} + 2\frac{du}{\overline{u}} \tag{B7}$$

## Correlation Equations

In the application of equations (B5), (B6), and (B7) to turbulent flow, the restriction is that the maximum deviations from the mean are small, since the derivatives are replaced by the corresponding turbulent fluctuation quantities. These equations can, nevertheless, be manipulated in various ways depending on what data are available and which terms are considered negligible. The following development is for the present situation where data for $\rho'$ and $p_t'$ are available and $p'/\overline{p}$ or $\overline{p'^2}/\overline{p}^2$ are generally negligible compared with other terms.

By first neglecting the pressure term $dp/\overline{p}$ in equation (B5), squaring the resulting equation, and taking the time mean, the following expression is obtained:

$$\frac{\overline{T_t'^2}}{\overline{T}^2} = \frac{\overline{\rho'^2}}{\overline{\rho}^2} - 2a\frac{\overline{\rho'u'}}{\overline{\rho}\overline{u}} + a^2\frac{\overline{u'^2}}{\overline{u}^2} \tag{B8}$$

In this equation $a = (\gamma - 1)\overline{M}^2$. Equating this result to the square of equation (B6) then gives

$$\frac{\overline{\rho'^2}}{\overline{\rho}^2} - 2a\frac{\overline{\rho'u'}}{\overline{\rho}\overline{u}} + \left(a^2 - b^2\right)\frac{\overline{u'^2}}{\overline{u}^2} = 0 \tag{B9}$$

where $b = n\left(1 + \frac{\gamma - 1}{2}\overline{M}^2\right)\left(1 - \frac{T_w}{T_t}\right)$. By squaring and taking the time mean of equation (B7), another relation between $\rho'$ and $u'$ is obtained as

$$\frac{\overline{u'^2}}{\bar{u}^2} = \frac{1}{4}\left(\frac{\overline{p_t'^2}}{\bar{p}_t^2} - \frac{\overline{\rho'^2}}{\bar{\rho}^2}\right) - \frac{\overline{\rho'u'}}{\bar{\rho}\bar{u}} \tag{B10}$$

Equations (B9) and (B10) are then solved for the two unknowns $\overline{\rho'u'}/\bar{\rho}\bar{u}$ and $\overline{u'^2}/\bar{u}^2$ to give the following expressions:

$$\frac{\overline{\rho'u'}}{\bar{\rho}\bar{u}} = \frac{\dfrac{\overline{\rho'^2}}{\bar{\rho}^2} + \dfrac{1}{4}(a - b)^2\left(\dfrac{\overline{p_t'^2}}{\bar{p}_t^2} - \dfrac{\overline{\rho'^2}}{\bar{\rho}^2}\right)}{a^2 - b^2 + 2a} \tag{B11}$$

$$\frac{\overline{u'^2}}{\bar{u}^2} = \frac{1}{a^2 - b^2 + 2a}\left[\frac{a}{2}\left(\frac{\overline{p_t'^2}}{\bar{p}_t^2} - \frac{\overline{\rho'^2}}{\bar{\rho}^2}\right) - \frac{\overline{\rho'^2}}{\bar{\rho}^2}\right] \tag{B12}$$

The coefficient

$$A = \frac{\overline{\rho'u'}}{\sqrt{\overline{\rho'^2}}\sqrt{\overline{u'^2}}} = \frac{\overline{\rho'u'}}{\bar{\rho}\bar{u}} \frac{\bar{\rho}}{\sqrt{\overline{\rho'^2}}} \frac{\bar{u}}{\sqrt{\overline{u'^2}}}$$

can then be evaluated and, as an indication of the reliability and consistency of the data, the values of $A$ should be within the limits $0 \leqq A \leqq 1.0$ which were mentioned previously. Examination of equation (B12) shows that for $\dfrac{T_w}{T_t} \ll 1.0$, corresponding to very cold wall conditions, negative values of $\overline{u'^2}/\bar{u}^2$ are predicted for $n \geqq 2.0$. For the conditions of reference 6 where the minimum $T_w/T_t$ was about 0.09, it therefore seems reasonable to restrict $n$ to the range $1.0 < n < 2.1$.

## Application to Data

Values of the correlation coefficient $A$ for the four runs of reference 6 as used herein have been computed from equations (B11) and (B12) for $n = 1.6$ and $n = 1.8$. All these data gave values in the range $0.4 < A < 4.5$ for $\frac{y}{\delta} > 0.1$. Since values of $A > 1.0$ are not physically possible, it can be assumed that data scatter is responsible for these large values. The equations thus predict that for these values of $n$, $0.4 < A < 1.0$. It is therefore justifiable to assume $A$ is constant, whereupon equation (B10) becomes quadratic in $\sqrt{\overline{u'^2}}/\bar{u}$ and equation (9) of the text is obtained. Values of $A$ in this range have been used to compute $\sqrt{\overline{u'^2}}/\bar{u}$ from equation (9) for one of the runs of reference 6, and

the results are shown in figure 15. It can be seen that the maximum effect on the pre-dicted values of $\sqrt{\overline{u'^2}}/\overline{u}$ over this range of values for $A$ is about $\pm 0.01$.

# APPENDIX C

## POSSIBLE EFFECTS OF THIRD-ORDER CORRELATIONS

After a reasonable range of values is established for the second-order correlation coefficient A, then possible effects of third-order correlations on the values of the predicted root-mean-square velocity fluctuations may be examined.

If the same procedure used in the text to derive equation (9) is followed, except that all terms consisting of up to third-order products of fluctuation quantities are retained, the following equation is obtained:

$$\frac{\overline{u'^2}}{\bar{u}^2} + \frac{\overline{u'q'^2}}{\bar{u}^3} + 2\frac{\overline{\rho'u'^2}}{\bar{\rho}\bar{u}^2} + \frac{1}{2}\frac{\overline{\rho'q'^2}}{\bar{\rho}\bar{u}^2} + \frac{\overline{\rho'^2u'}}{\bar{\rho}^2\bar{u}} = \frac{1}{4}\left(\frac{\overline{p_t'^2}}{\bar{p}_t^2} - \frac{\overline{\rho'^2}}{\bar{\rho}^2}\right) - \frac{\overline{\rho'u'}}{\bar{\rho}\bar{u}} \tag{C1}$$

Comparison of this result with equation (B10) shows that four third-order terms that involve $u'$, $\rho'$, and the fluctuating velocity vector $q' = (u'^2 + v'^2 + w'^2)^{1/2}$ have been added. In order to write an explicit expression for $U = \frac{\sqrt{\overline{u'^2}}}{\bar{u}}$, the third-order correlation coefficients are defined as

$$\left. \begin{aligned}
R_{uq^2} &= \frac{\overline{u'q'^2}}{\sqrt{\overline{u'^2}}\;\overline{q'^2}} \approx \frac{\overline{u'q'^2}}{c(\overline{u'^2})^{3/2}} \\[2ex]
R_{\rho u^2} &= \frac{\overline{\rho'u'^2}}{\sqrt{\overline{\rho'^2}}\;\overline{u'^2}} \\[2ex]
R_{\rho q^2} &= \frac{\overline{\rho'q'^2}}{\sqrt{\overline{\rho'^2}}\;\overline{q'^2}} \approx \frac{\overline{\rho'q'^2}}{c\sqrt{\overline{\rho'^2}}\;\overline{u'^2}} \\[2ex]
R_{\rho^2 u} &= \frac{\overline{\rho'^2u'}}{\overline{\rho'^2}\sqrt{\overline{u'^2}}}
\end{aligned} \right\} \tag{C2}$$

where $c = \frac{\overline{q'^2}}{\overline{u'^2}}$. Introduction of these coefficients into equation (C1) gives the following cubic equation for U:

$$cR_{uq^2}U^3 + \left(1 + 2R_{\rho u^2}r + \frac{c}{2}R_{\rho q^2}r\right)U^2 + \left(Ar + R_{\rho^2 u}r^2\right)U - \frac{1}{4}\left(P^2 - r^2\right) = 0 \tag{C3}$$

# APPENDIX C

Since the sign and exact magnitude of the third-order coefficients are unknown, the best that can be done at present is to obtain solutions to equation (C3) for a range of constant values assigned to the third-order correlation coefficients. These solutions have been carried out with $A = 1.0$ and $c = 2$ (as used in ref. 13). The range of values used for the four third-order correlation coefficients was varied independently from -1.0 to 1.0 corresponding to perfect anticorrelation and perfect correlation. The results are shown for a typical run in figure 15. When $\dfrac{\sqrt{u'^2}}{\bar{u}} \approx 0.1$, the effect of these coefficients is maximized at about ±20 percent. When $\dfrac{\sqrt{u'^2}}{\bar{u}} \approx 0.02$, the effect is less, as would be expected, and amounts to about ±10 percent. The predicted values of $\sqrt{u'^2}/\bar{u}$ were the largest when all coefficients were -1.0 and the smallest when all coefficients were +1.0. Since these particular combinations of limiting values are not likely, it can be concluded that unless the intensity of velocity fluctuations considerably exceeds 0.1, the third-order correlations are indeed negligible.

# REFERENCES

1. Morkovin, Mark V.: Effects of Compressibility on Turbulent Flows. The Mechanics of Turbulence, Gordon and Breach Science Publ., c.1964, pp. 367-380.

2. Kovásznay, Leslie S. G.: Turbulence in Supersonic Flow. J. Aeronaut. Sci., vol. 20, no. 10, Oct. 1953, pp. 657-674, 682.

3. Kistler, Alan L.: Fluctuation Measurements in a Supersonic Turbulent Boundary Layer. Phys. Fluids, vol. 2, no. 3, May-June 1959, pp. 290-296.

4. Muntz, E. P.: Gas Density Fluctuations in the Hypersonic Turbulent Wake of a Sharp, Slender Cone. BSD-TR 67-28, U.S. Air Force, Feb. 1967.

5. Lien, Hwachii; and Eckerman, Jerome: Interferometric Analysis of Density Fluctuations in Hypersonic Turbulent Wakes. AIAA J., vol. 4, no. 11, Nov. 1966, pp. 1988-1994.

6. Wallace, J. E.: Hypersonic Turbulent Boundary Layer Measurements Using an Electron Beam. CAL Rep. No. AN-2112-Y-1 (NASA Contract No. NSR33-009-029), Cornell Aeronaut. Lab., Inc., Aug. 1968.

7. Hurle, I. R.; Russo, A. L.; and Hall, J. Gordon: Spectroscopic Studies of Vibrational Nonequilibrium in Supersonic Nozzle Flows. J. Chem. Phys., vol. 40, no. 8, Apr. 1964, pp. 2076-2089.

8. Rust, J. H.; and Sesonske, Alexander: Turbulent Temperature Fluctuations in Mercury and Ethylene Glycol in Pipe Flow. Int. J. Heat Mass Transfer, vol. 9, no. 3, Mar. 1966, pp. 215-227.

9. Escudier, M. P.; and Spalding, D. B.: A Note on the Turbulent Uniform-Property Hydrodynamic Boundary Layer on a Smooth Impermeable Wall; Comparisons of Theory With Experiment. Brit. A.R.C. 27 302, Aug. 1965.

10. Maise, George; and McDonald, Henry: Mixing Length and Kinematic Eddy Viscosity in a Compressible Boundary Layer. AIAA J., vol. 6, no. 1, Jan. 1968, pp. 73-80.

11. Glushko, G. S.: Turbulent Boundary Layer on a Flat Plate in an Incompressible Fluid. Bull. Acad. Sci. USSR, Mech. Ser., no. 4, 1965, pp. 13-23.

12. Bradshaw, P.; Ferriss, D. H; and Atwell, N. P.: Calculation of Boundary-Layer Development Using the Turbulent Energy Equation. J. Fluid Mech., vol. 28, pt. 3, May 26, 1967, pp. 593-616.

13. Beckwith, Ivan E.; and Bushnell, Dennis M. (With appendix C by Carolyn C. Thomas): Detailed Description and Results of a Method for Computing Mean and Fluctuating Quantities in Turbulent Boundary Layers. NASA TN D-4815, 1968.

14. Harvey, William D.; and Bushnell, Dennis M.: Velocity Fluctuation Intensities in a Hypersonic Turbulent Boundary Layer. AIAA J. (Tech. Notes), vol. 7, no. 4, Apr. 1969, pp. 760-762.

15. Danberg, James E.: Measurement of the Characteristics of the Compressible Turbulent Boundary Layer With Air Injection. NAVORD Rep. 6683, U.S. Nav. Ord. Lab., Sept. 3, 1959.

16. Speaker, W. V.; and Ailman, C. M.: Static and Fluctuating Pressures in Regions of Separated Flow. AIAA Paper No. 66-456, June 1966.

17. Laufer, John: Some Statistical Properties of the Pressure Field Radiated by a Turbulent Boundary Layer. Phys. Fluids, vol. 7, no. 8, Aug. 1964, pp. 1191-1197.

18. Lilley, G. M.: Wall Pressure Fluctuations Under Turbulent Boundary Layers at Subsonic and Supersonic Speeds. AGARD Rep. 454, Apr. 1963.

19. Klebanoff, P. S.: Characteristics of Turbulence in a Boundary Layer With Zero Pressure Gradient. NACA Rep. 1247, 1955. (Supersedes NACA TN 3178.)

20. Serafini, John S.: Wall-Pressure Fluctuations and Pressure-Velocity Correlations in a Turbulent Boundary Layer. NASA TR R-165, 1964.

21. Townsend, A. A.: The Structure of the Turbulent Boundary Layer. Proc. Cambridge Phil. Soc., vol. 47, pt. 2, Apr. 1951, pp. 375-395.

22. Jonsson, V. K.; and Batton, W. D.: Hot-Wire Anemometer Study of a Turbulent Boundary Layer on a Porous Axial Circular Cylinder With Uniform Air Injection. HTL-TR-65 (AFOSR 65-2724), Univ. of Minnesota, Sept. 1965. (Available from DDC as AD 628 083.)

23. Schubauer, G. B.; and Klebanoff, P. S.: Investigation of Separation of the Turbulent Boundary Layer. NACA Rep. 1030, 1951. (Supersedes NACA TN 2133.)

24. Schubauer, G. B.; and Klebanoff, P. S.: Contributions on the Mechanics of Boundary-Layer Transition. NACA Rep. 1289, 1956. (Supersedes NACA TN 3489.)

25. Smith, Kenneth A.: The Transpired Turbulent Boundary Layer. Ph. D. Thesis, Massachusetts Inst. Technol., 1962.

26. Johnson, Donald S.: Turbulent Heat Transfer in a Boundary Layer With Discontinuous Wall Temperature. Pub. No. 55(OSR Tech. Note 55-289), Dep. Aero., The Johns Hopkins Univ., Aug. 1955.

27. Kline, S. J.; Lisin, A. V.; and Waitman, B. A.: Preliminary Experimental Investigation of Effect of Free-Stream Turbulence on Turbulent Boundary-Layer Growth. NASA TN D-368, 1960.

28. Escudier, Marcel Paul:  The Turbulent Incompressible Hydrodynamic Boundary Layer.  Ph. D. Thesis, Univ. of London, 1967.

29. Sandborn, Virgil A.; and Braun, Willis H.:  Turbulent Shear Spectra and Local Isotropy in the Low-Speed Boundary Layer.  NACA TN 3761, 1956.

30. Mull, Harold R.; and Algranti, Joseph S.:  Flight Measurement of Wall-Pressure Fluctuations and Boundary-Layer Turbulence.  NASA TN D-280, 1960.

31. Schloemer, Howard H.:  Effects of Pressure Gradients on Turbulent Boundary-Layer Wall-Pressure Fluctuations.  USL Rep. No. 747, U.S. Navy, July 1, 1966.

32. Chowdhury, Shamsuzzaman:  Turbulent Eddies in Boundary Layers on Smooth and Rough Flat Plate.  CER65SC-EJP57 (Res. Grant DA-AMC-28-043-G20), Colorado State Univ., Mar. 1966.  (Available from DDC as AD 633915.)

33. Tieleman, Henry W.:  Viscous Region of Turbulent Boundary Layer.  CER67-68HWT21 (Res. Grant DA-AMC-28-043-65-G20), Colorado State Univ., Dec. 1967.  (Available from DDC as AD 665 393.)

34. Wooldridge, C. E.; and Muzzy, R. J.:  Boundary-Layer Turbulence Measurements With Mass Addition and Combustion.  AIAA J., vol. 4, no. 11, Nov. 1966, pp. 2009-2016.

35. Klebanoff, P. S.; and Diehl, Z. W.:  Some Features of Artificially Thickened Fully Developed Turbulent Boundary Layers With Zero Pressure Gradient.  NACA Rep. 1110, 1952.  (Supersedes NACA TN 2475.)

36. Runstadler, P. W.; Kline, S. J.; and Reynolds, W. C.:  An Experimental Investigation of the Flow Structure of the Turbulent Boundary Layer.  AFOSR-TN-5241, U.S. Air Force, June 1963.  (Available from DDC as AD 421683.)

37. Willmarth, W. W.; and Wooldridge, C. E.:  Measurements of the Fluctuating Pressure at the Wall Beneath a Thick Turbulent Boundary Layer.  02920-1-T (Contract No. Nonr-1224(30)), College Eng., Univ. of Michigan, Apr. 1962.

38. Liu, C. K.; Kline, S. J.; and Johnston, J. P.:  An Experimental Study of Turbulent Boundary Layer on Rough Walls.  Rep. MD-15 (AFOSR 67-0420), Stanford Univ., July 1966.  (Available from DDC as AD 647 268.)

39. Watson, Ralph D.; and Cary, A. M., Jr.:  The Transformation of Hypersonic Turbulent Boundary Layers to Incompressible Form.  AIAA J. (Tech. Notes), vol. 6, no. 6, June 1967, pp. 1202-1203.

40. Sternberg, Joseph:  The Transition From a Turbulent to a Laminar Boundary Layer.  Rep. No. 906, Ballistic Res. Lab., Aberdeen Proving Ground, May 1954.

41. Demetriades, Anthony:  Turbulent Fluctuation Measurement in Compressible, Axisymmetric Wakes.  AIAA J. (Tech. Notes), vol. 5, no. 5, May 1967, pp. 1028-1029.

42. Truitt, Robert Wesley:  Hypersonic Aerodynamics.  Ronald Press Co., c.1959.

43. Norris, John D.:  Calibration of Conical Pressure Probes for Determination of Local Flow Conditions at Mach Numbers From 3 to 6.  NASA TN D-3076, 1965.

44. Wuest, W.:  Pressure Measuring Probes in Aerodynamic Research Technology. Aerodynamic Measurement Technology — Proceedings of the First Meeting of the Subcommittee on Aerodynamic Measuring Technology, NASA TT F-11856, 1969, pp. 41-83.

45. Lowson, M. V.:  Pressure Fluctuations in Turbulent Boundary Layers.  NASA TN D-3156, 1965.
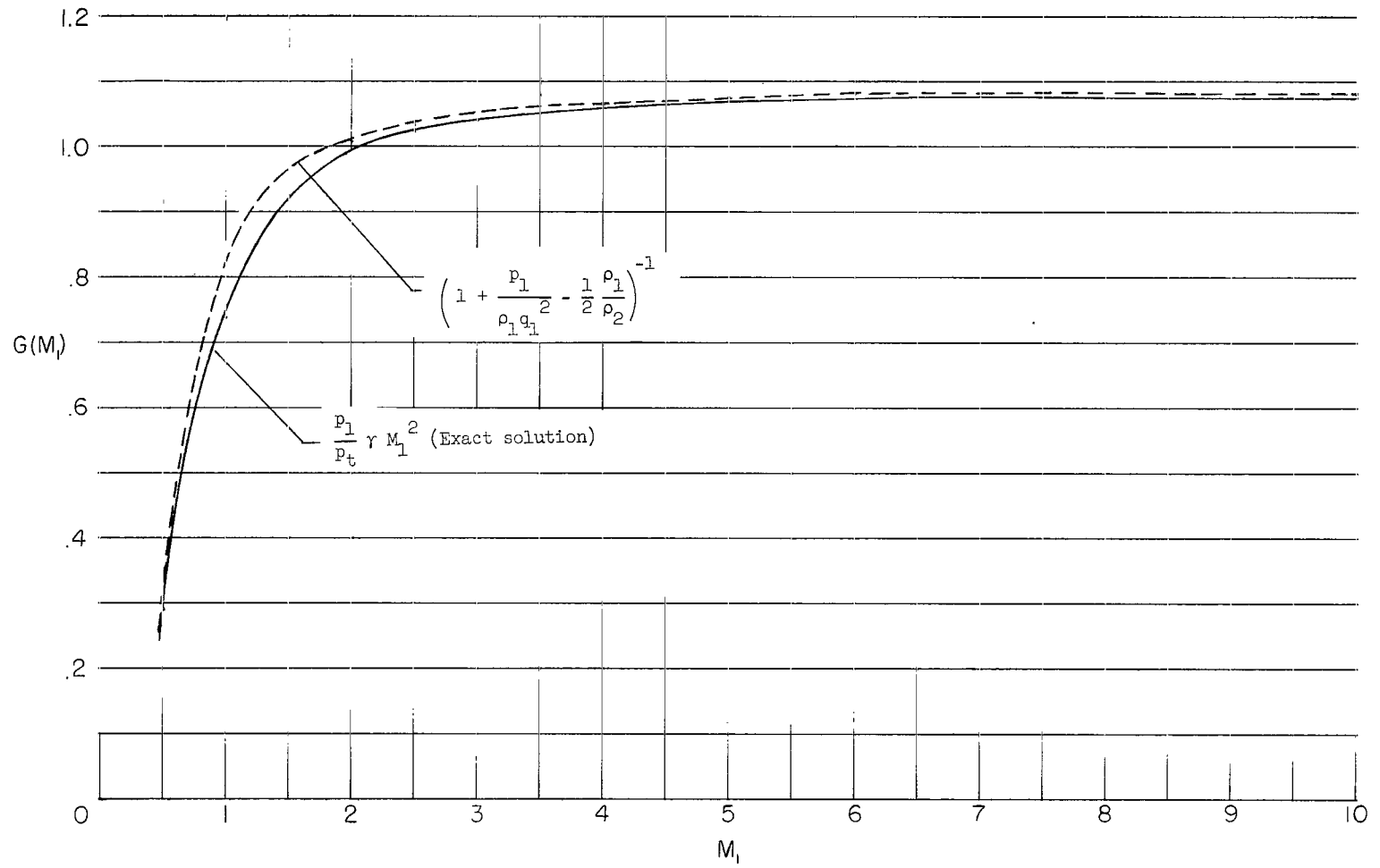
Figure 1.- Comparison of exact and approximate expressions for the variable function of Mach number. $\gamma = 7/5$.

The figure plots $G(M_1)$ versus $M_1$. Two curves are shown:

$$\left(1 + \frac{p_1}{\rho_1 q_1^{\ 2}} - \frac{1}{2}\frac{\rho_1}{\rho_2}\right)^{-1}$$

$$\frac{p_1}{p_t}\gamma M_1^{\ 2} \ \text{(Exact solution)}$$

| | | $M_e$ | $R_\delta$ | $T_o$, $^\circ R$ ($^\circ K$) | $h_w/H_o$ | $\delta$, in. (cm) |
|---|---|---|---|---|---|---|
| —— | ◯ | 8.62 | $5.37 \times 10^4$ | 3793 (2107) | 0.12 | 5.9 (15.0) |
| ———— | ☐ | 8.25 | 6.68 | 5800 (3222) | .07 | 5.2 (13.2) |
| — — | ◇ | 8.82 | 8.46 | 3592 (1996) | .13 | 5.5 (14.0) |
| ———· | △ | 8.89 | 10.75 | 2918 (1621) | .16 | 5.9 (15.0) |



Figure 2.- Distribution of measured density fluctuations.

| $M_e$ | $R_\delta$ | $T_o$, $^\circ R$ ($^\circ K$) | $h_w/H_o$ | $\delta$, in. (cm) |
|---|---|---|---|---|
| ———○ 8.62 | $5.37 \times 10^4$ | 3793 (2107) | 0.12 | 5.9 (15.0) |
| ———□ 8.25 | 6.68 | 5800 (3222) | .07 | 5.2 (13.2) |
| ——◇ 8.82 | 8.46 | 3592 (1996) | .13 | 5.5 (14.0) |
| ———△ 8.89 | 10.75 | 2918 (1621) | .16 | 5.9 (15.0) |

Solid symbols for measured $\sqrt{p_w'^2}/\bar{p}_w$
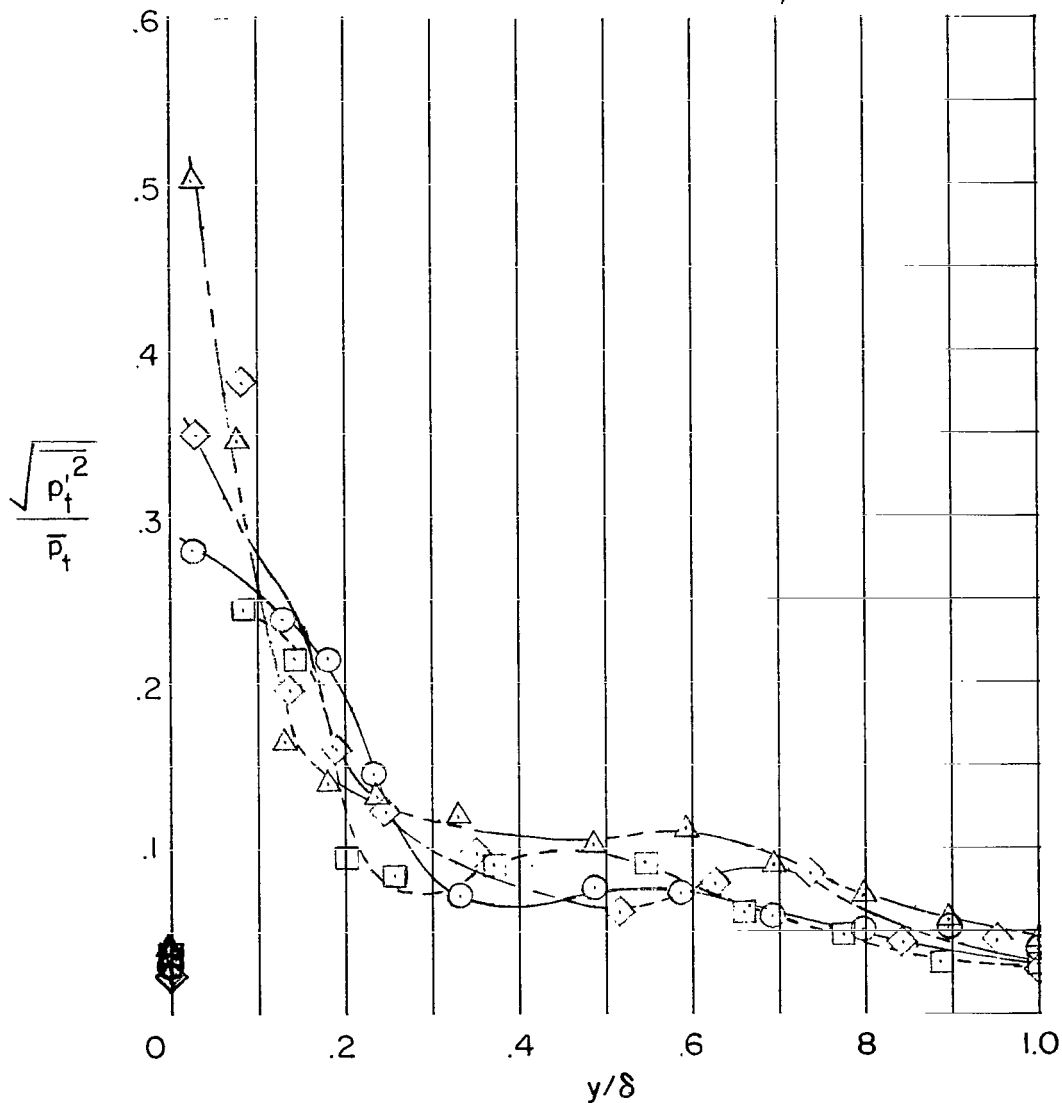
(a) Measured pitot-pressure fluctuations.

Figure 3.- Pressure-fluctuation distributions.

33

$12 \times 10^{-3}$

$10$

$8$

$\dfrac{\sqrt{\overline{p_w'^2}}}{\frac{1}{2}\rho_e u_e^2}$ $6$

$4$

$2$

○ ⊙ ■ ☐ ◁ △ } Data presented in reference 16 from other sources

● Speaker and Ailman (ref. 16)
—— Laufer (ref. 17)
△ Wallace (ref. 6)
---- Correlation equation (12)

Adiabatic-wall-temperature conditions

Cold-wall-temperature conditions of reference 6

$O$ $2$ $4$ $6$ $8$ $10$ $12$

$M_e$
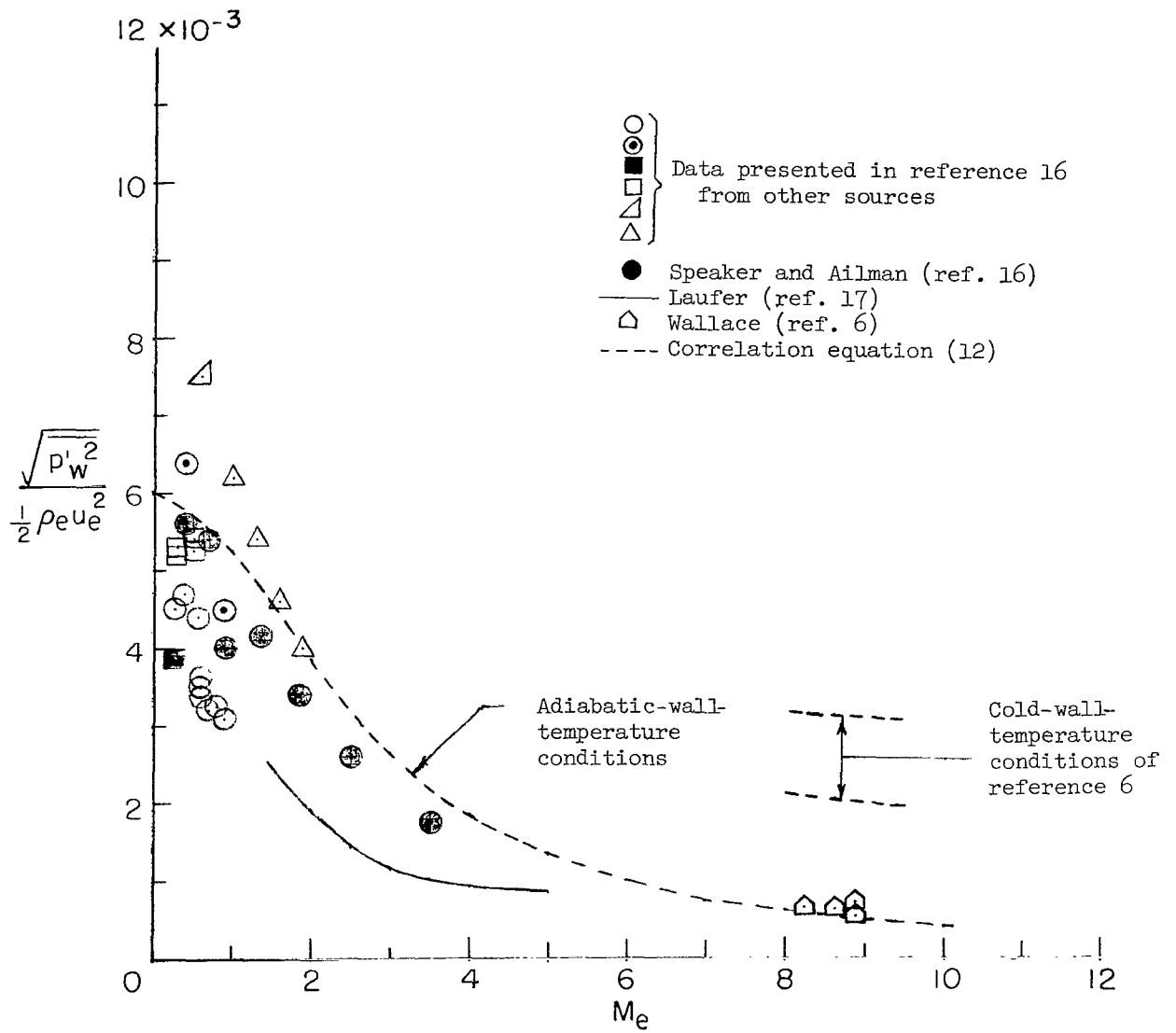
(b) Comparison of wall-pressure fluctuations in turbulent boundary layer.

Figure 3.- Concluded.

34

$\dfrac{\bar{\rho}}{\rho_e}$

| | $M_e$ | $R_\delta$ | $T_o$, $^\circ R$ ($^\circ K$) | $h_w/H_o$ | $\delta$, in. (cm) |
|---|---|---|---|---|---|
| ——O | 8.62 | $5.37 \times 10^4$ | 3793 (2107) | 0.12 | 5.9 (15.0) |
| ———□ | 8.25 | 6.68 | 5800 (3222) | .07 | 5.2 (13.2) |
| —·—◇ | 8.82 | 8.46 | 3592 (1996) | .13 | 5.5 (14.0) |
| —··—△ | 8.89 | 10.75 | 2918 (1621) | .16 | 5.9 (15.0) |

$y/\delta$
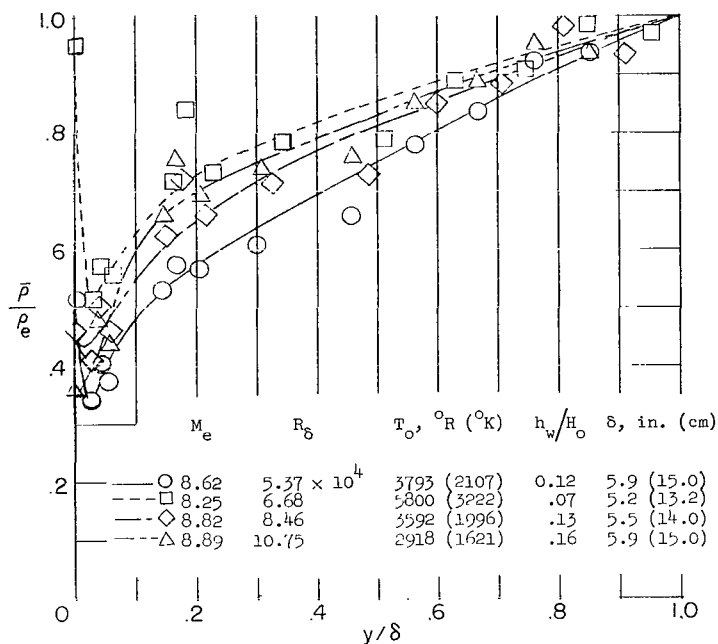
(a) Fairing from reference 6.

$\dfrac{\bar{\rho}}{\rho_e}$

$y/\delta$
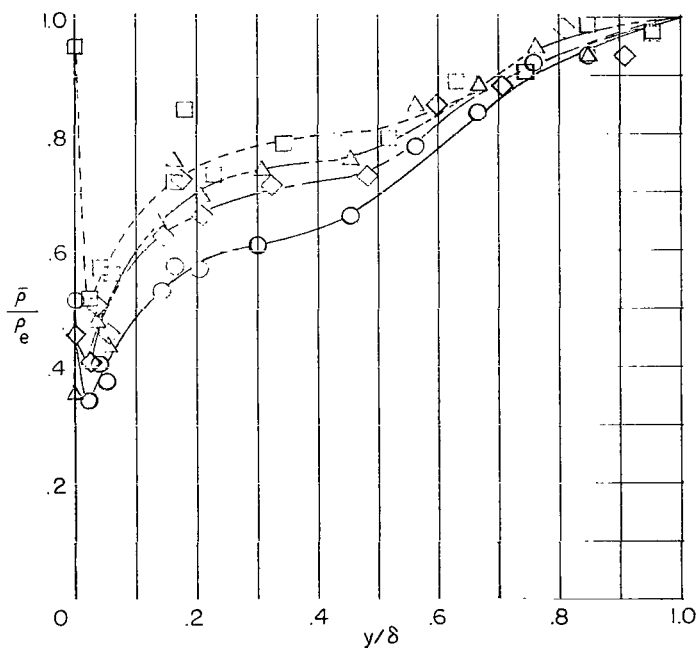
(b) Present fairing.

Figure 4.- Mean-density profiles.

35

| $M_e$ | $R_\delta$ | $h_w/H_o$ | $\delta$, in. (cm) |
|---|---|---|---|
| 8.25 to 8.89 | 5.37 to 10.75 $\times$ 10$^4$ | 0.07 to 0.16 | 5.2 to 5.9 (13.2 to 15.0) |
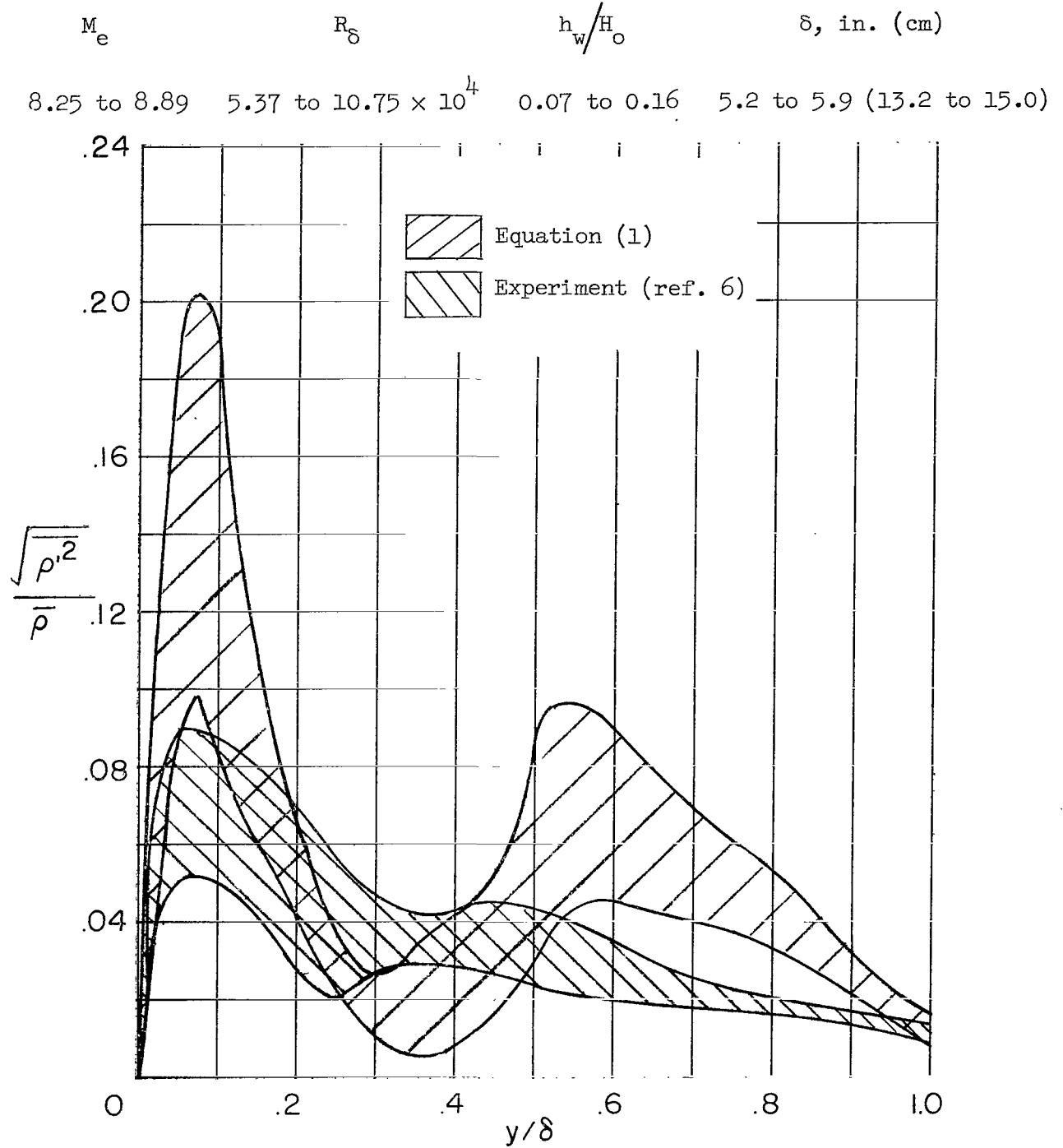
Figure 5.- Intensity of density fluctuations.
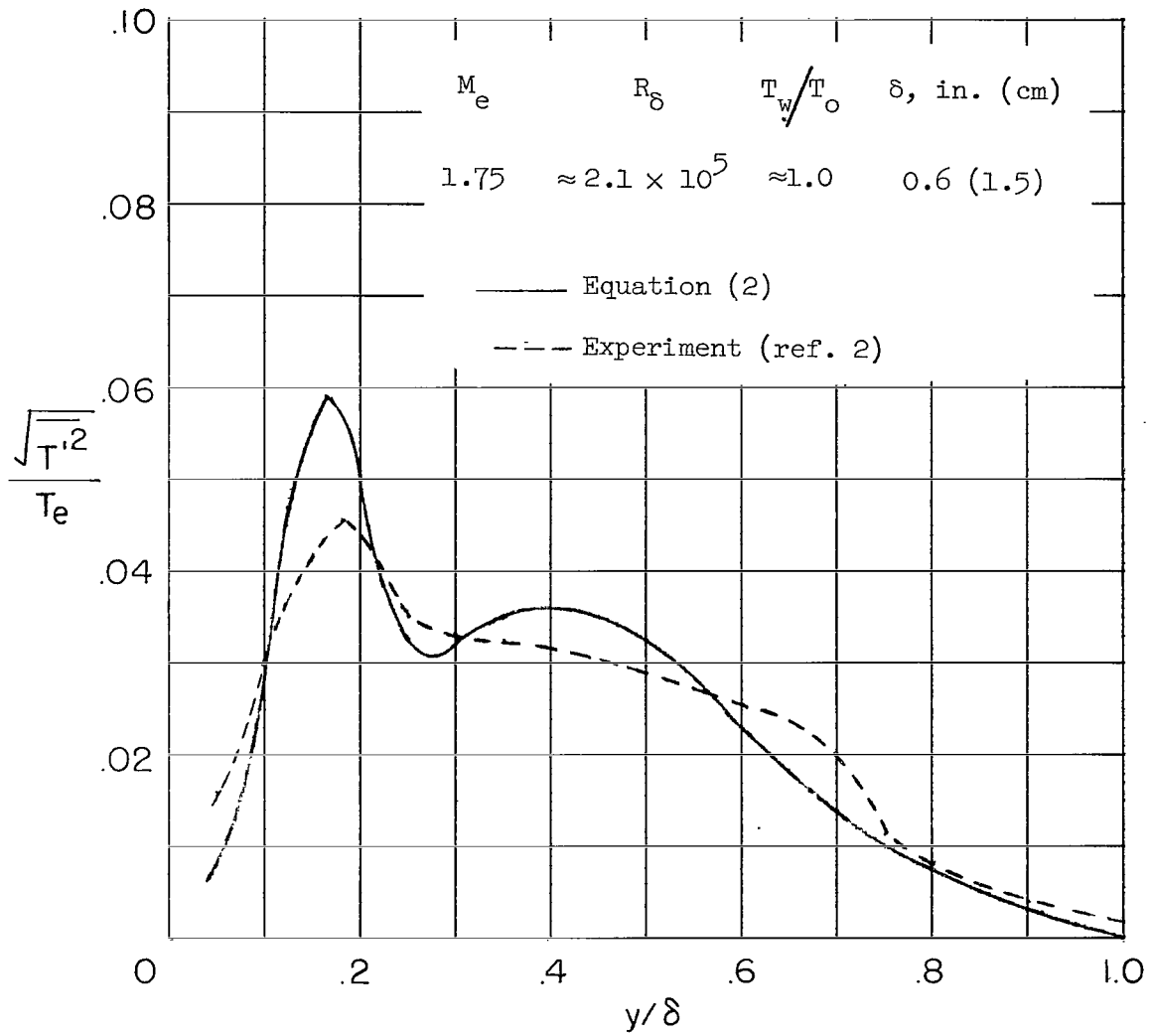
(a) Comparison with data from reference 2.

Figure 6.- Comparison of mixing-length calculations with measured fluctuating temperatures from previous experiments (refs. 2 and 3).
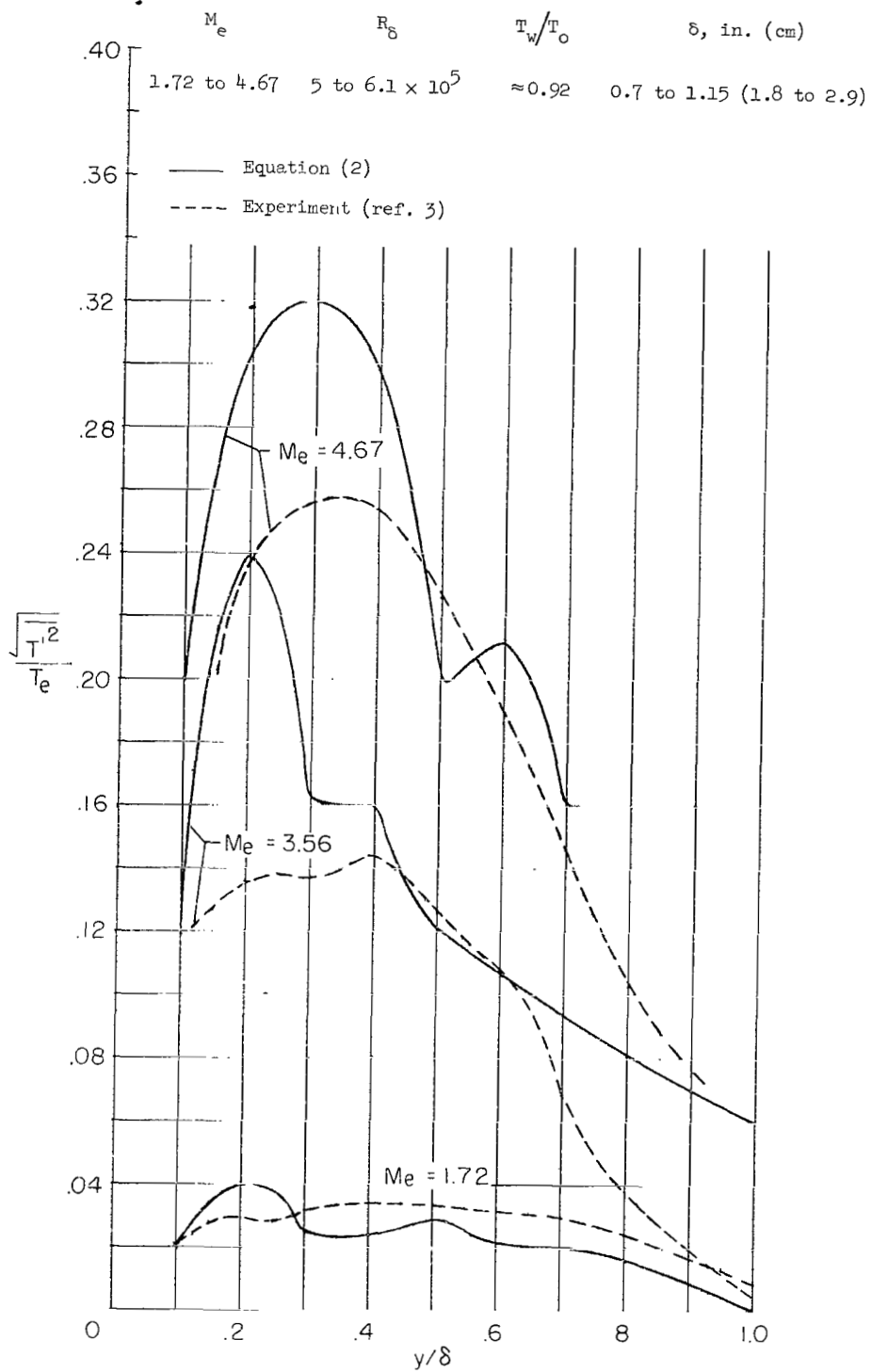
(b) Comparison with data from reference 3.

Figure 6.- Concluded.
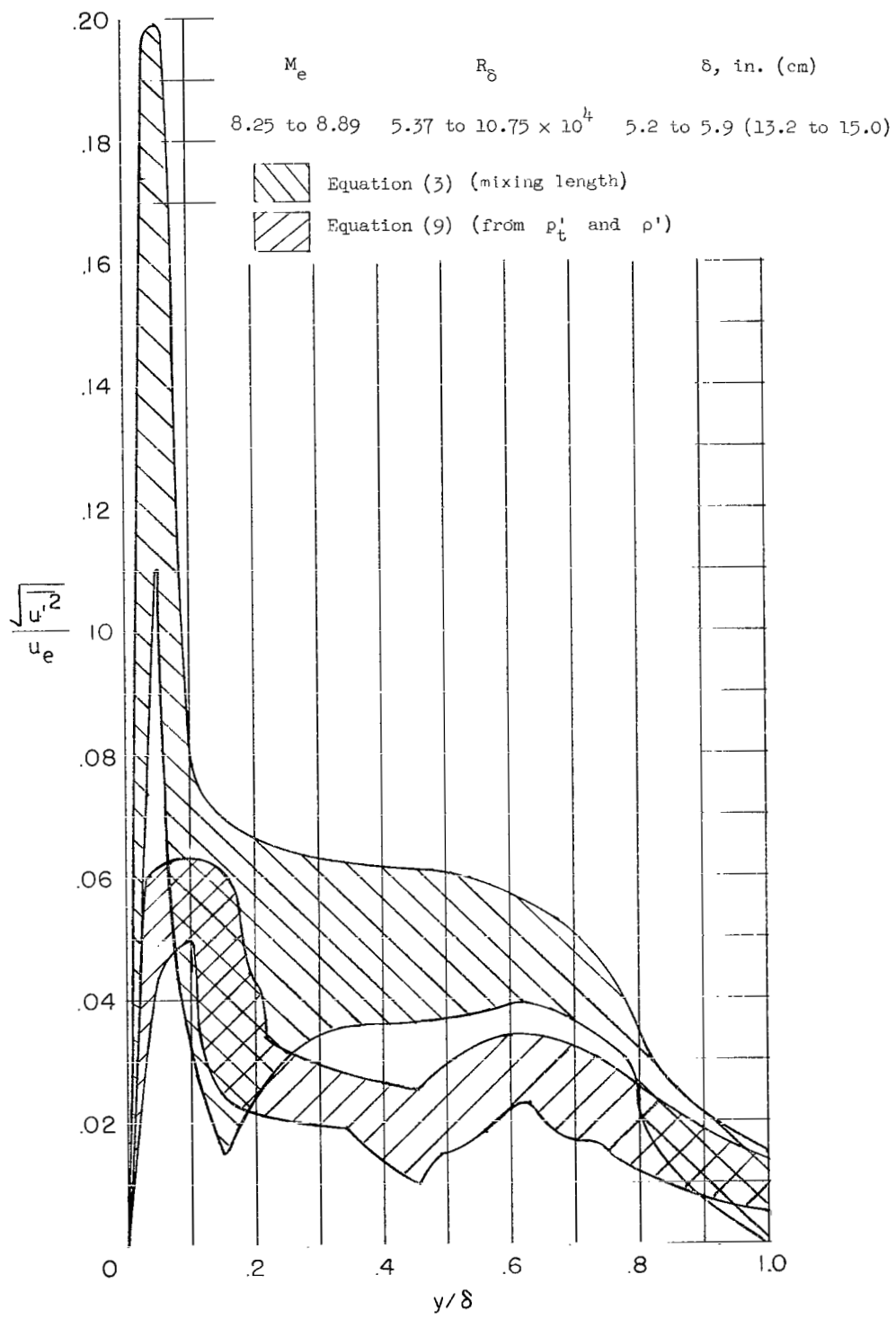
Figure 7.- Comparison of present fluctuating velocities computed from equations (3) and (9).
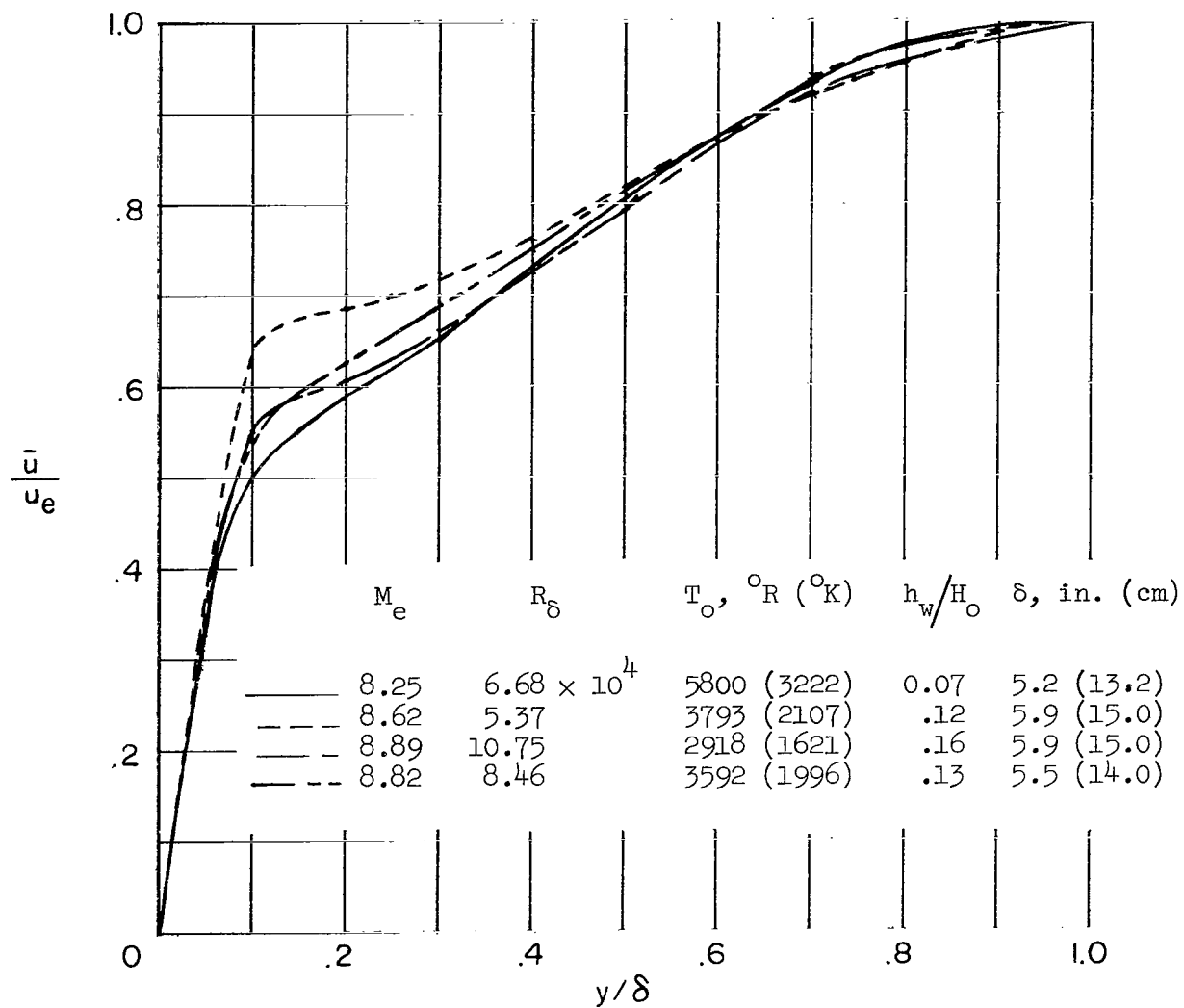
Figure 8.- Mean-velocity profiles.
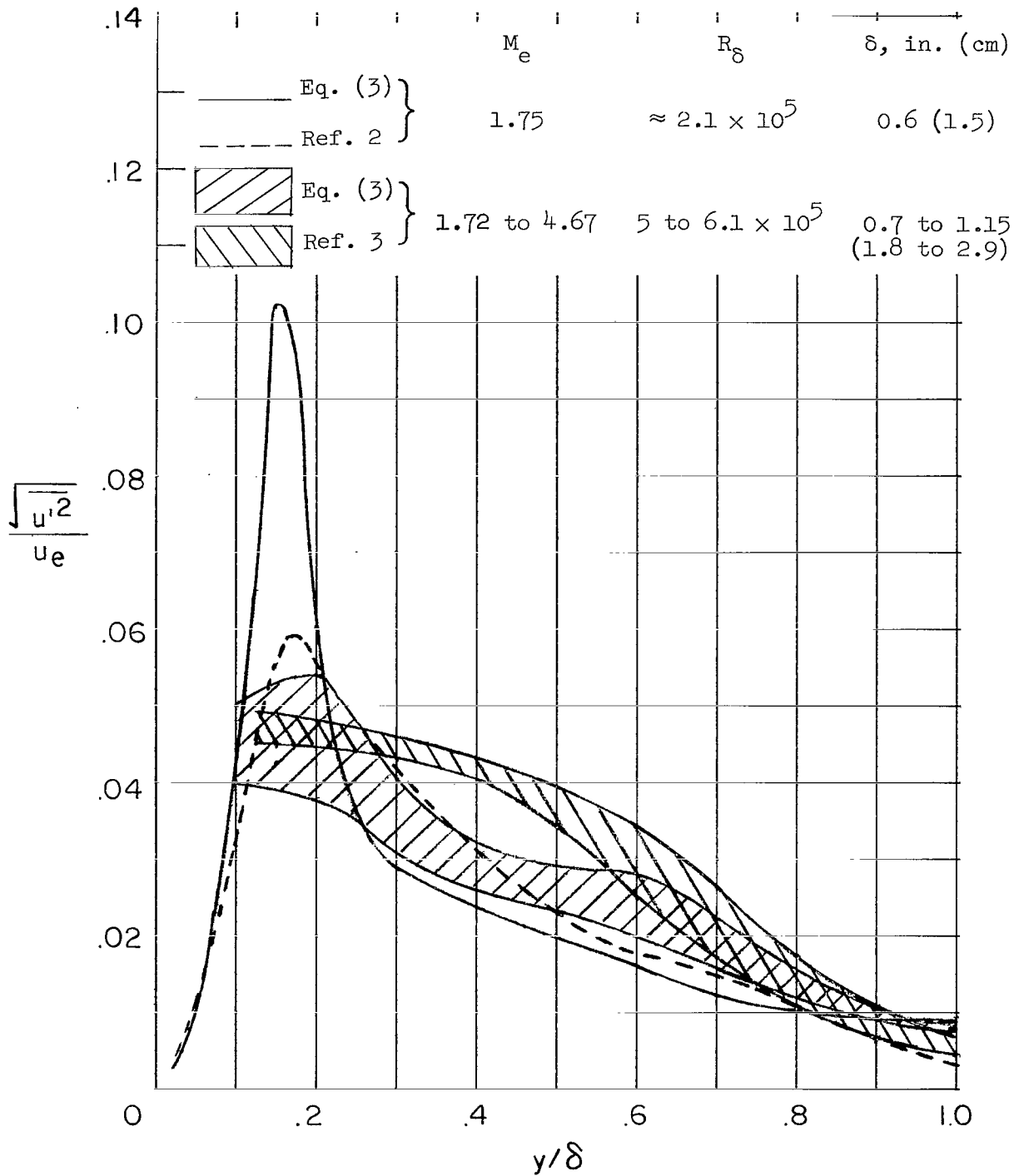
Figure 9.- Comparison of measured fluctuating velocity from previous experiments (refs. 2 and 3) with mixing-length calculations (eq. (3)).
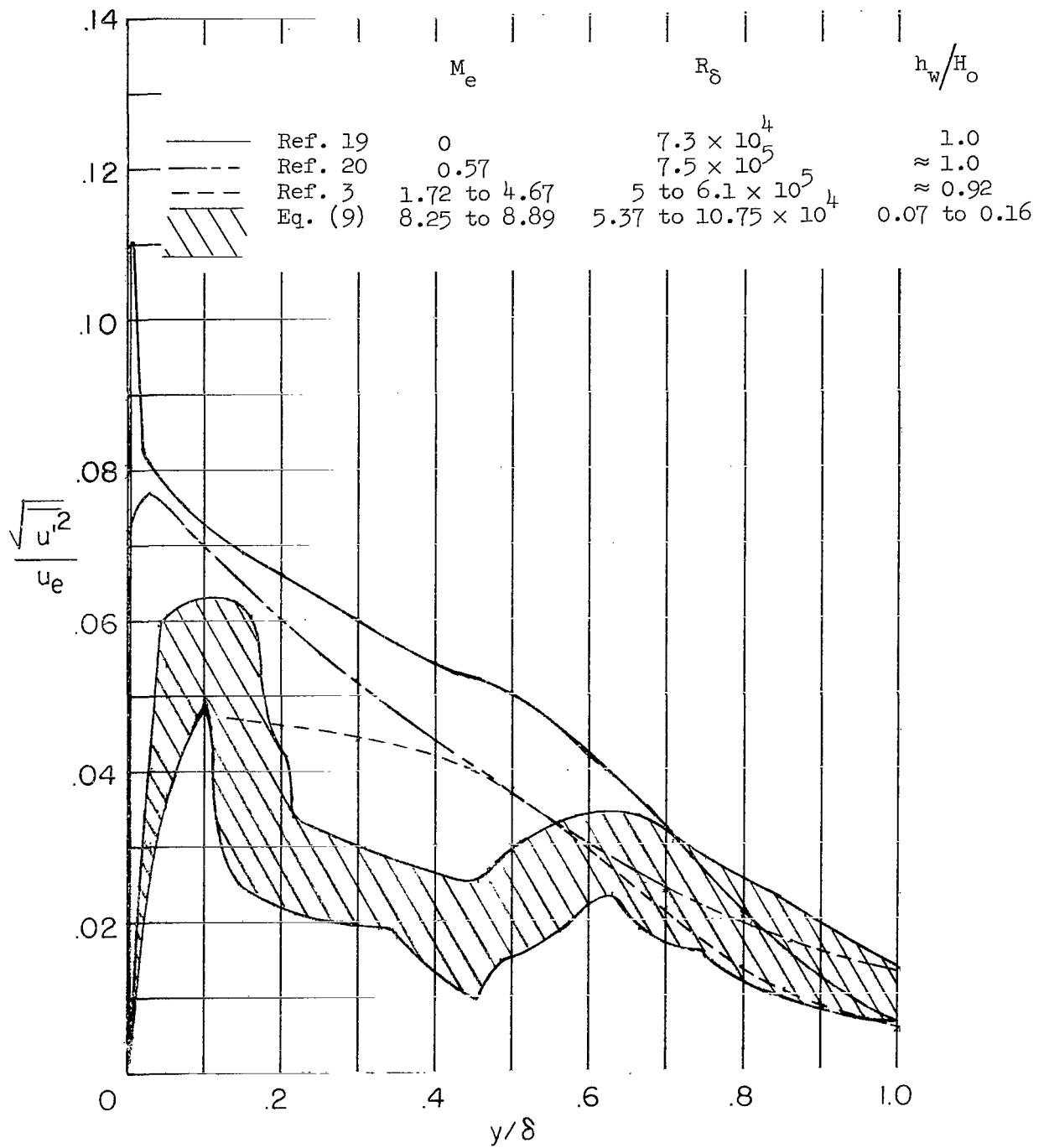
Figure 10.- Comparison of present velocity fluctuation intensity with previous results.
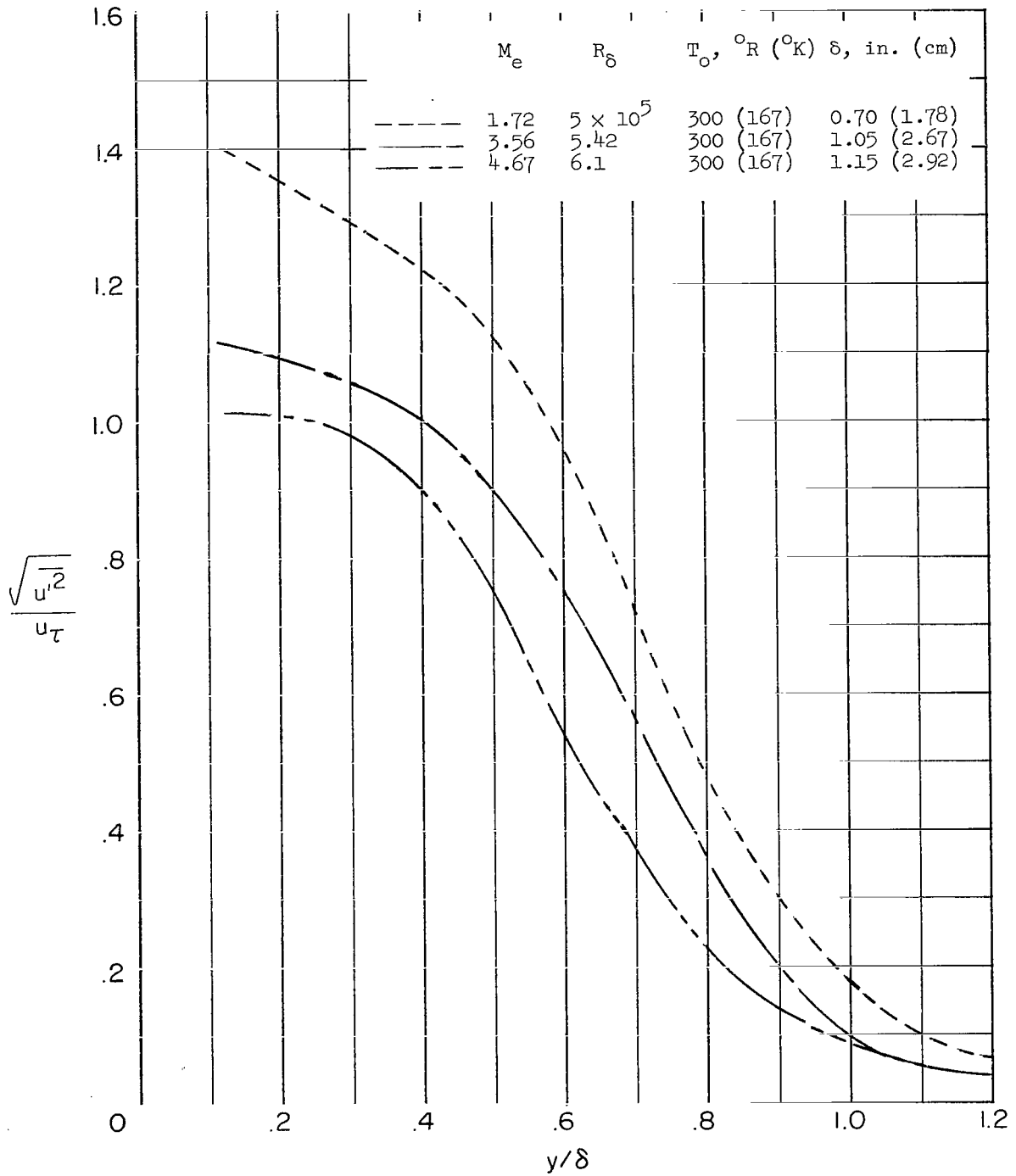
(a) Normalized by shear-stress velocity.

Figure 11.- Fluctuating velocity through turbulent boundary layer (taken from ref. 3).
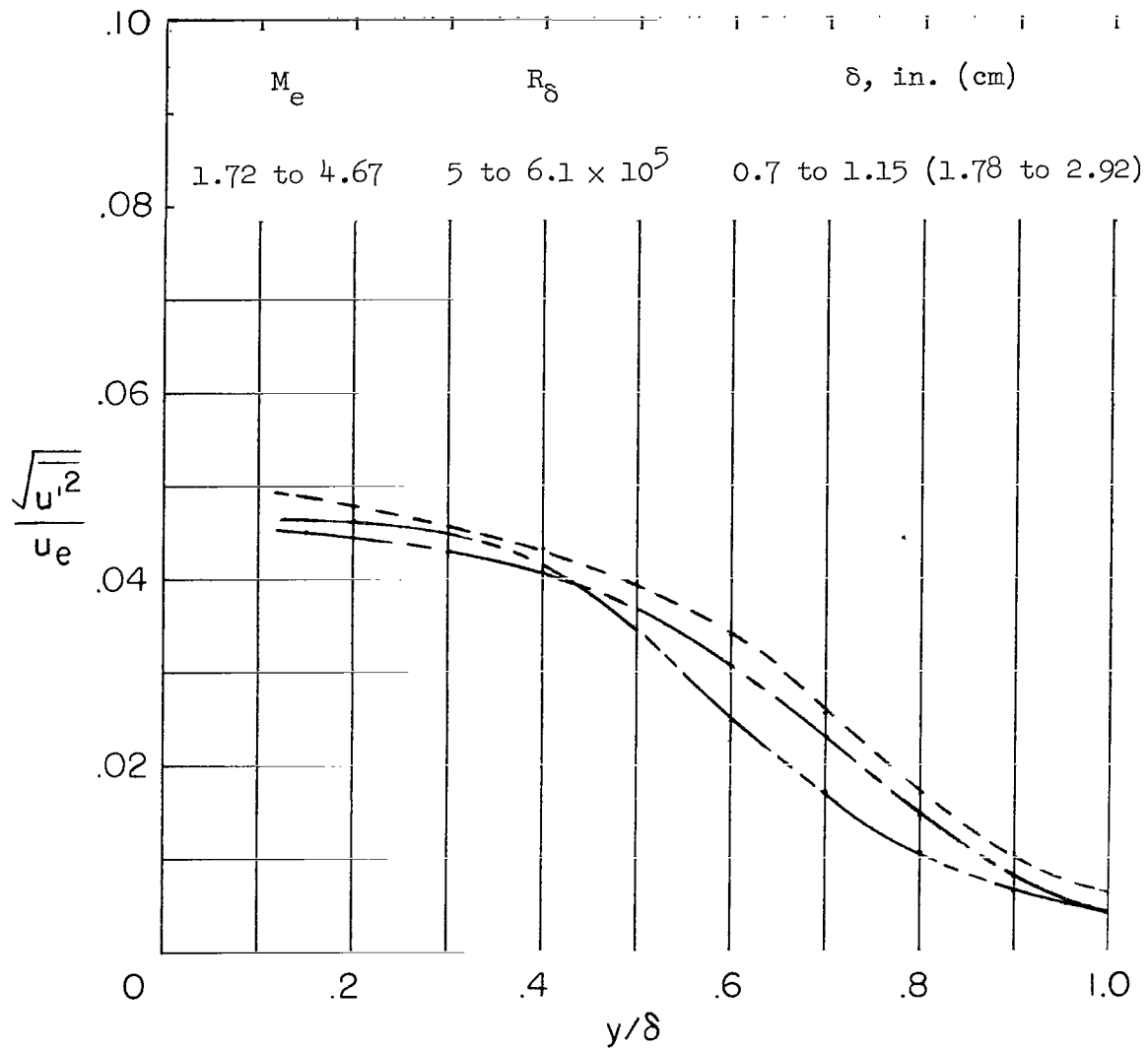
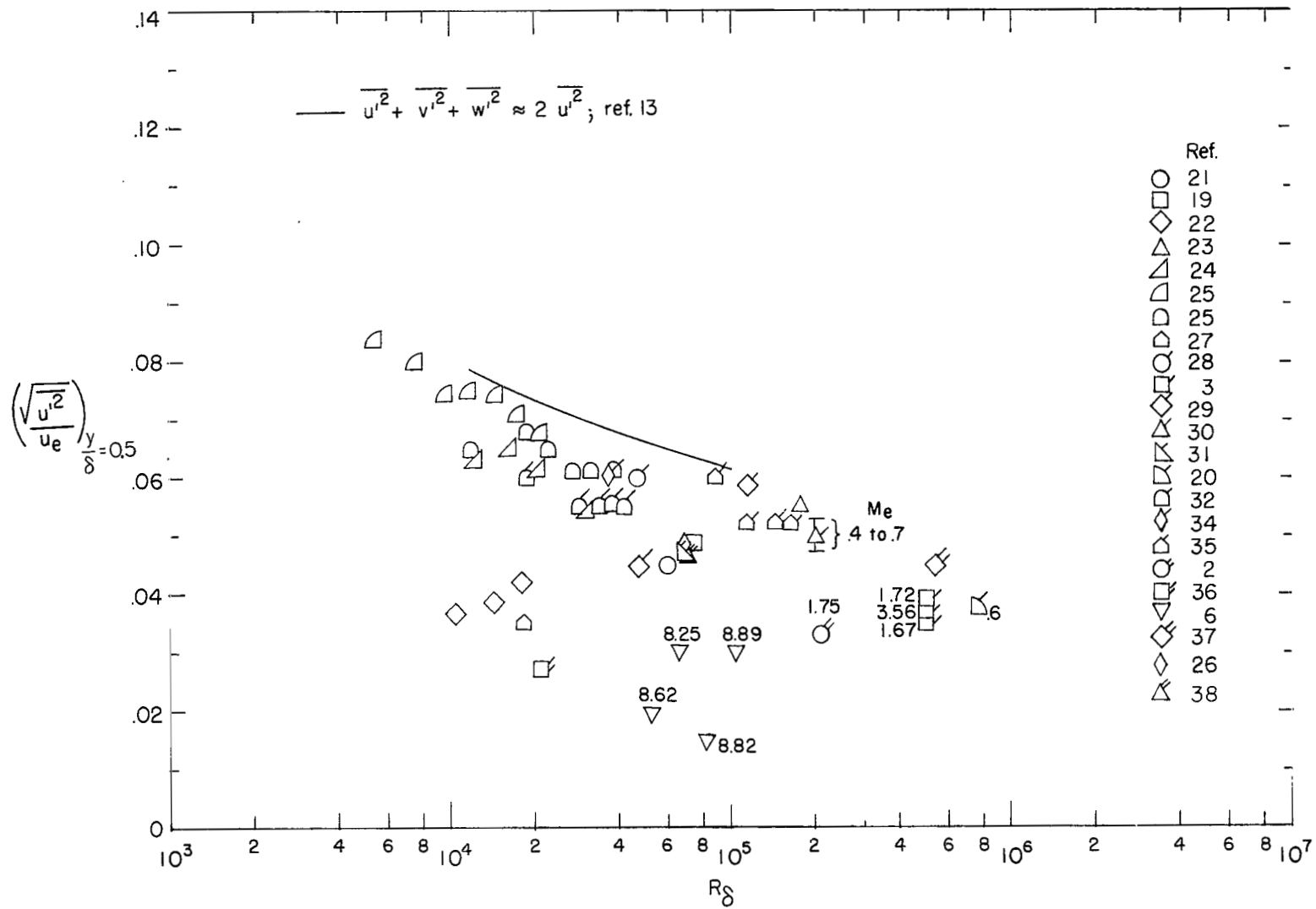(b) Normalized by $u_e$.

Figure 11.- Concluded.
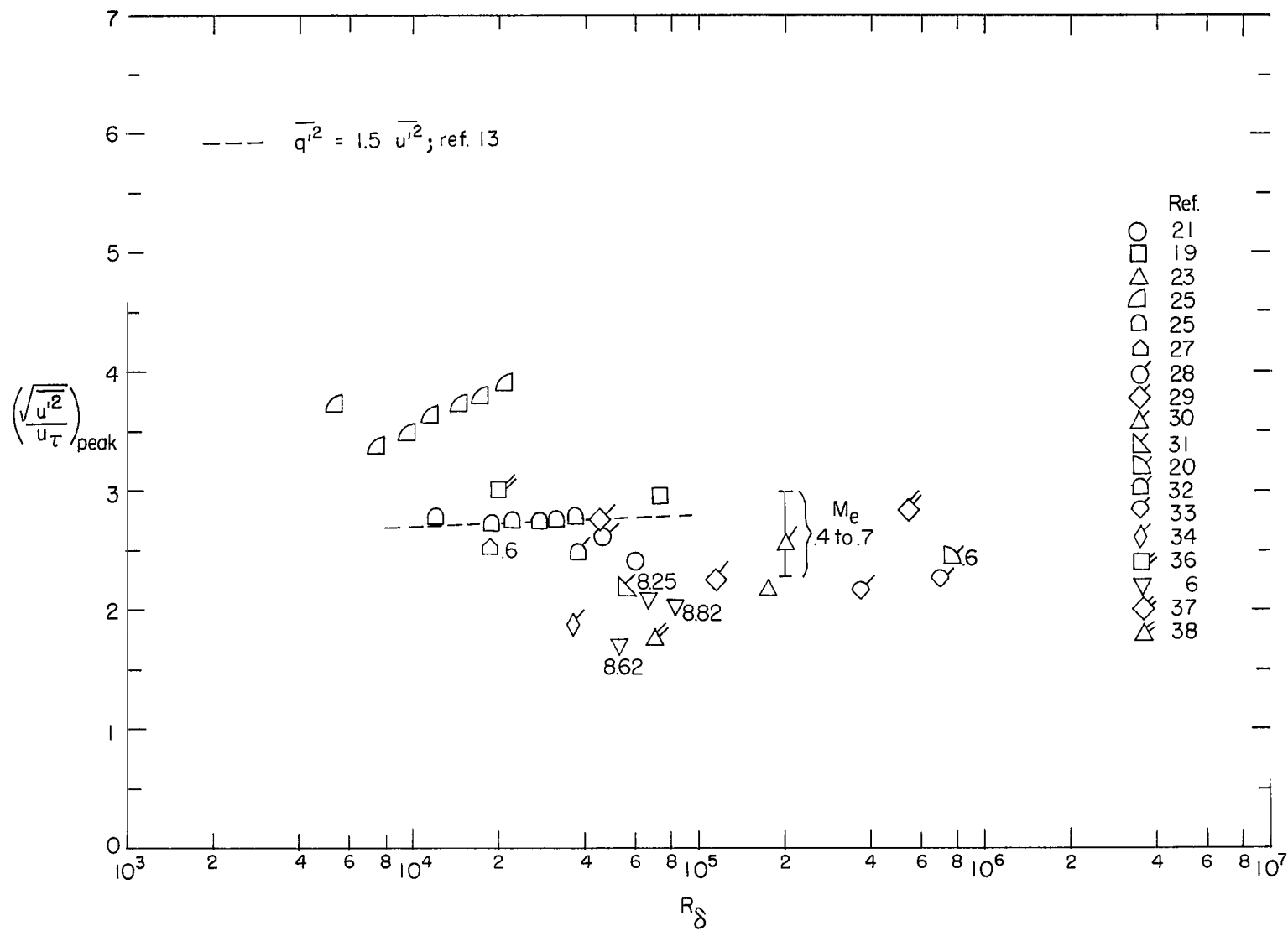
(a) Peak velocity fluctuation normalized by $u_\tau$.

Figure 12.- Longitudinal turbulence intensity, with $\delta$ chosen for $\frac{u}{u_e} = 0.995$. $\frac{dp}{dx} = 0$.
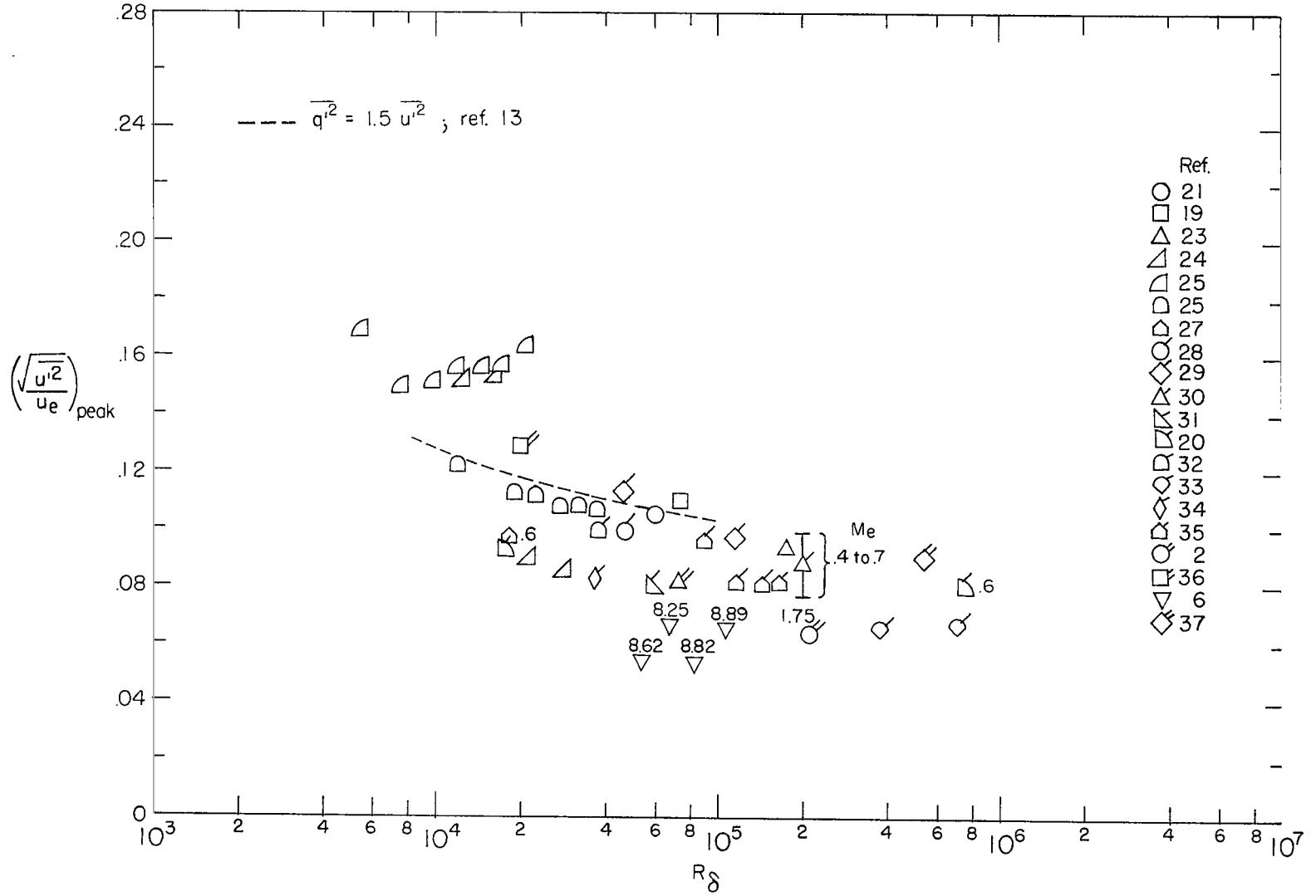
(b) Peak velocity fluctuation normalized by $u_e$.

Figure 12.- Continued.

(c) Velocity fluctuation (normalized by $u_e$) at $\frac{y}{\delta} = 0.5$.
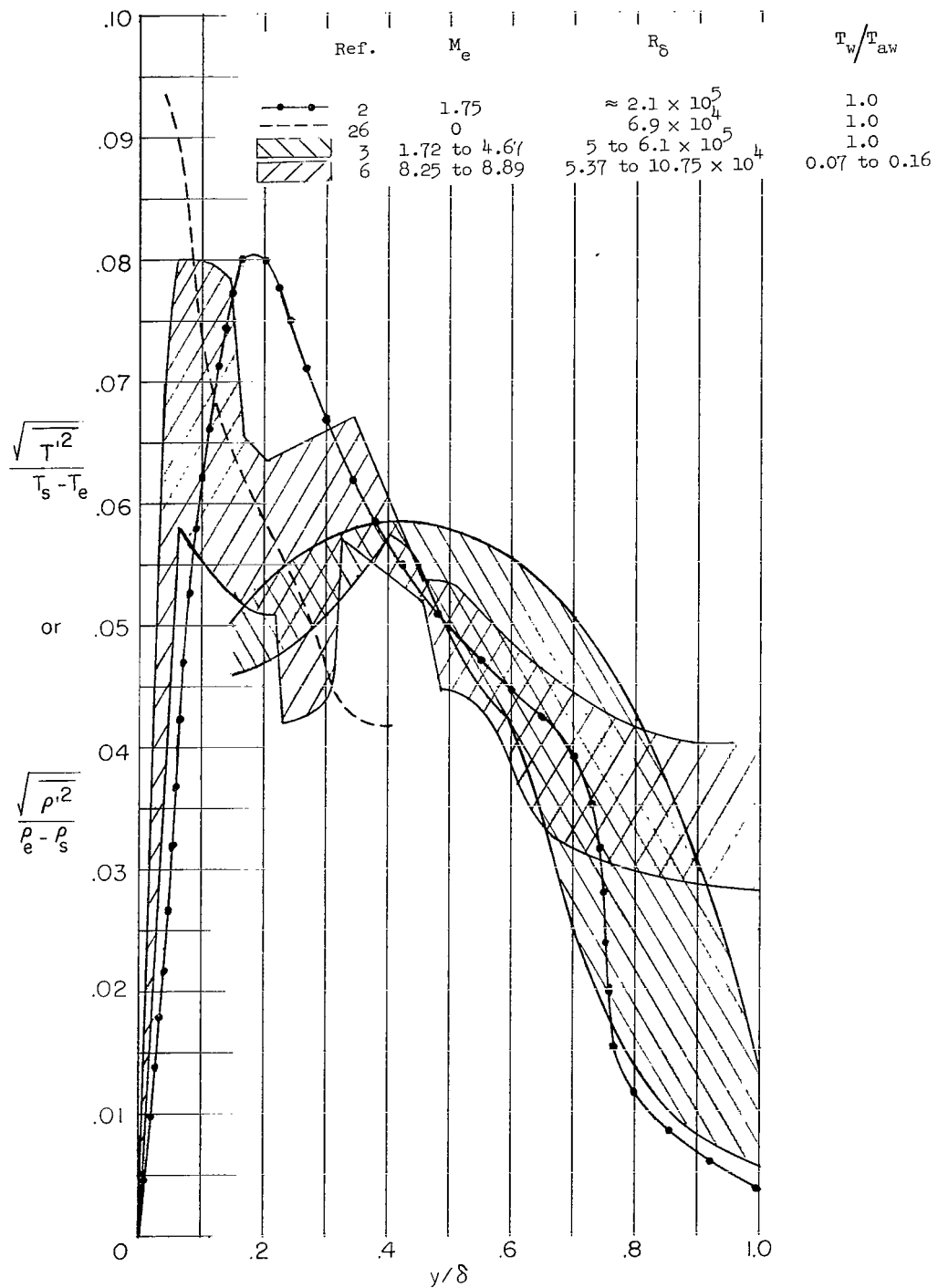
Figure 12.- Concluded.

| | Ref. | $M_e$ | $R_\delta$ | $T_w/T_{aw}$ |
|---|---|---|---|---|
| ●—●—● | 2 | 1.75 | $\approx 2.1 \times 10^5$ | 1.0 |
| — — — | 26 | 0 | $6.9 \times 10^4$ | 1.0 |
| ⬛⬛⬛ | 3 | 1.72 to 4.67 | 5 to $6.1 \times 10^5$ | 1.0 |
| ⬜⬜⬜ | 6 | 8.25 to 8.89 | 5.37 to $10.75 \times 10^4$ | 0.07 to 0.16 |

$\dfrac{\sqrt{\overline{T'^2}}}{T_s - T_e}$

or

$\dfrac{\sqrt{\overline{\rho'^2}}}{\rho_e - \rho_s}$

$y/\delta$

Figure 13.– Temperature and density fluctuations normalized by their respective defects. $\dfrac{dp}{dx} = 0$. (Data from refs. 2, 3, and 26 are for temperature and data from ref. 6 are for density.)
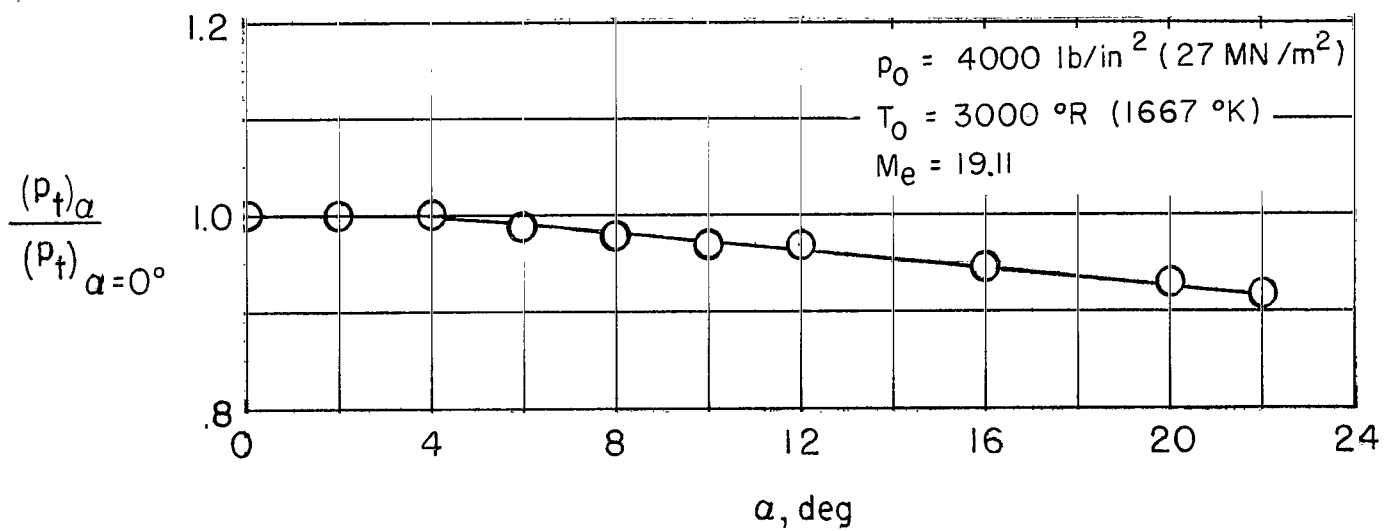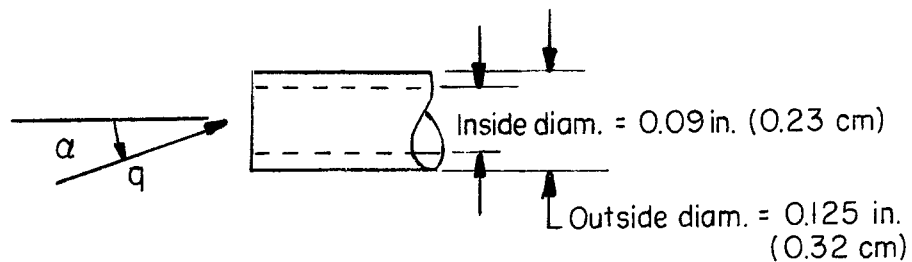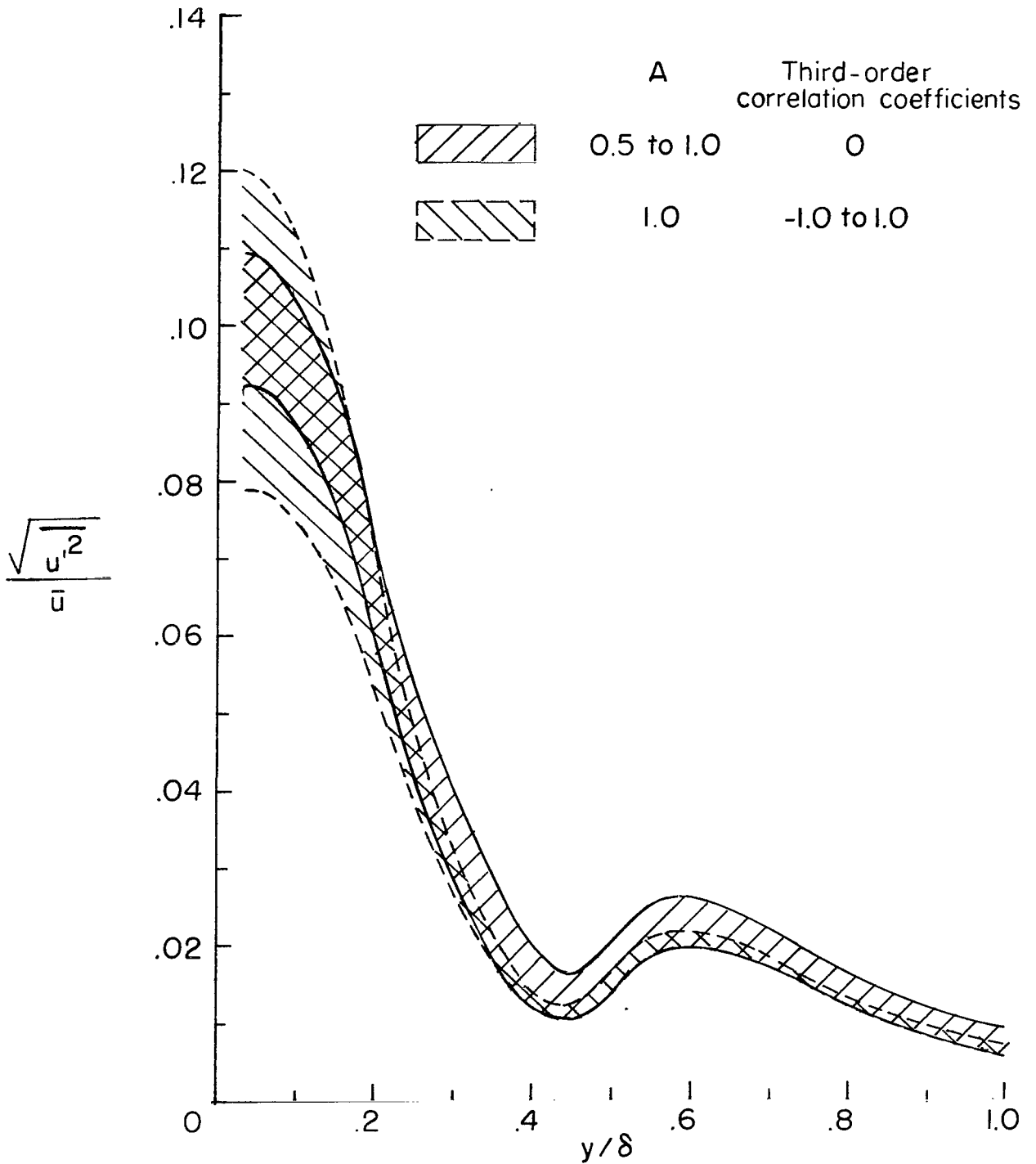
Figure 14.- Effect of angle of attack on pitot pressure.

Figure 15.- Effect of second- and third-order correlation coefficients on $\sqrt{u'^2}/\overline{u}$ for one run of reference 6 at a free-stream Reynolds number per foot (per 30.5 cm) of $1.10 \times 10^5$. $T_0 = 3790^\circ$ R $(2106^\circ$ K$)$; $p_0 = 240$ lb/in$^2$ $(1.65$ MN/m$^2)$; $c = 2.0$.

**FIRST CLASS MAIL**

06U 001 37 '1 30S           69266   00903
AIR FORCE WEAPONS LABORATORY/WLIL/
KIRTLAND AIR FORCE BASE, NEW MEXICC 87111

ATT E. LOU BOWMAN, CHIEF,TECH. LIBRARY

*"The aeronautical and space activities of the United States shall be
conducted so as to contribute . . . to the expansion of human knowl-
edge of phenomena in the atmosphere and space. The Administration
shall provide for the widest practicable and appropriate dissemination
of information concerning its activities and the results thereof."*

— NATIONAL AERONAUTICS AND SPACE ACT OF 1958

# NASA SCIENTIFIC AND TECHNICAL PUBLICATIONS

**TECHNICAL REPORTS:** Scientific and
technical information considered important,
complete, and a lasting contribution to existing
knowledge.

**TECHNICAL NOTES:** Information less broad
in scope but nevertheless of importance as a
contribution to existing knowledge.

**TECHNICAL MEMORANDUMS:**
Information receiving limited distribution
because of preliminary data, security classifica-
tion, or other reasons.

**CONTRACTOR REPORTS:** Scientific and
technical information generated under a NASA
contract or grant and considered an important
contribution to existing knowledge.

**TECHNICAL TRANSLATIONS:** Information
published in a foreign language considered
to merit NASA distribution in English.

**SPECIAL PUBLICATIONS:** Information
derived from or of value to NASA activities.
Publications include conference proceedings,
monographs, data compilations, handbooks,
sourcebooks, and special bibliographies.

**TECHNOLOGY UTILIZATION
PUBLICATIONS:** Information on technology
used by NASA that may be of particular
interest in commercial and other non-aerospace
applications. Publications include Tech Briefs,
Technology Utilization Reports and Notes,
and Technology Surveys.

*Details on the availability of these publications may be obtained from:*

**SCIENTIFIC AND TECHNICAL INFORMATION DIVISION**

**NATIONAL AERONAUTICS AND SPACE ADMINISTRATION**
**Washington, D.C. 20546**